



## Marine Organic Aerosols at Mace Head: Effects from Phytoplankton and Source Region Variability

Emmanuel Chevassus<sup>1</sup>, Kirsten N. Fossum<sup>1</sup>, Darius Ceburnis<sup>1</sup>, Lu Lei<sup>1</sup>, Chunshui Lin<sup>1,2</sup>, Wei Xu<sup>1a</sup>, Colin D.O' Dowd<sup>1</sup>, Jurgita Ovadnevaite<sup>1</sup>

5 <sup>1</sup> School of Natural Sciences, Ryan Institute's Centre for Climate and Air Pollution Studies, University of Galway, Galway, Ireland

<sup>2</sup> Institute of Urban Environment, Chinese Academy of Sciences, Xiamen 361021

<sup>a</sup> Now at: State Key Laboratory of Loess and Quaternary Geology (SKLLQG), Center for Excellence in Quaternary Science and Global Change, Institute of Earth Environment, Chinese Academy of Sciences, Xi'an 10 710061, China

*Correspondence to:* Jurgita Ovadnevaite (jurgita.ovadnevaite@universityofgalway.ie)

### 2. Abstract

Organic aerosols (OA) are recognised as a significant component of particulate matter (PM), yet, their specific composition and sources, especially over remote areas remain elusive due to the overall scarcity of high-resolution online data. In this study, positive matrix factorisation was performed on organic aerosol mass spectra obtained from high-resolution time-of-flight aerosol mass spectrometer (HR-ToF-AMS) measurements to resolve sources contributing to the coastal PM. The focus was on a summertime period marked by enhanced biological productivity with prevailing pristine maritime conditions. Four OA factors were deconvolved by the source apportionment model. The analysis revealed primary marine organic aerosols (PMOA) as the predominant submicron OA at Mace Head during summertime, accounting for 42%. This was trailed by more oxidized oxygenated organic aerosols (MO-OOA) at 32%, methanesulphonic acid organic aerosols (MSA-OA) at 17%, and locally emitted peat-derived organic aerosols (Peat-OA) at 9% of the total OA mass. The total mass concentrations of primary organic aerosols and secondary organic aerosols were overall equal and almost exclusively present in the marine boundary layer consistently with previous findings. This study reveals that OA not only reflects atmospheric chemistry and meteorology – as evidenced by the significant aging of summertime polar air masses over the North Atlantic, driven by ozonolysis under Greenland anticyclonic conditions - but also serve as indicators of marine ecosystems. This is evident from MSA-OA being notably associated with stress enzyme markers and PMOA showing the typical makeup of largely abacterial phytoplankton extracellular metabolic processes. This study also reveals distinctive source regions within the North Atlantic Ocean for OA factors. MSA-OA is primarily associated with the Iceland Basin, with rapid production following coccolithophore blooms (lag of 1-2 days), while diatoms contribute to a slower formation process (lag of 9 days), reflecting distinct oceanic biological processes. In contrast, PMOA is sourced from more variable ecoregions, including the Southern Celtic Sea, West European Basin, and Newfoundland Basin, with additional contributions from chlorophytes and cyanobacteria at more southerly latitudes. Overall, these findings emphasise the need for further long-term investigation to fully account for phytoplankton's taxa variability influence on aerosol composition and their broader impacts on aerosol-climate interactions.

**Keywords:** Submicron Marine Aerosols, Secondary Organic Aerosols, HR-ToF-AMS, PMF, phytoplankton



## 1 Introduction

The marine environment plays a critical role in regulating climate through sea spray and gas-phase emissions from the oceans, via direct and indirect solar radiation effects and cloud formation governed by ocean biology, sea spray physicochemical properties and secondary reactions (Cochran *et al.*, 2017). However, aerosols in the atmospheric marine boundary layer (MBL) remain a significant source of uncertainty in radiative forcing estimates (Rosenfeld *et al.*, 2019; Wang *et al.*, 2020) primarily due to limited knowledge about aerosol mass, chemical composition, and particle number distributions (Carslaw *et al.*, 2017). Along with this, the origin of marine organic aerosols (OA), specifically whether formed by primary or secondary processes, requires further investigation.

Primary Marine Organic Aerosols (PMOA) consist of sea spray aerosols, produced by bursting bubbles, film, jet, and spume drops (Ovadnevaite *et al.* 2014; Veron 2015; Villermaux *et al.* 2022) that carry sea salt particles enriched in biogenic organic aerosols (O'Dowd *et al.* 2004; Facchini *et al.* 2008). The majority (80 %) of fine carbonaceous particles in the clean N.E Atlantic marine atmosphere has been shown to directly originate from phytoplankton activity as reported with dual carbon isotopes analysis (Ceburnis *et al.* 2011). The phytoplankton-OA link is particularly well-established, yet the topic is still highly debated as no clear full-picture consensus has been reached owing to widely changing temporal and geographic fluctuations (Lawler *et al.*, 2024; Lewis *et al.*, 2021; Seidel *et al.*, 2022). In addition, the specifics of how phytoplankton control OA chemical composition (Behrenfeld *et al.*, 2019; Facchini *et al.*, 2008; O'Dowd *et al.*, 2015), numbers flux (Markuszewski *et al.*, 2024; Sellegri *et al.*, 2023), size (Croft *et al.*, 2021; O'Dowd *et al.*, 2004; Saliba *et al.*, 2019), lifespan and surface tension (Lee *et al.*, 2020; Ovadnevaite *et al.*, 2017; Sellegri *et al.*, 2021) are all the focus of intense ongoing investigations.

In a warming world, following a high-emissions scenario (RCP8.5) trajectory, climate change is projected to drastically alter the geographic and seasonal variability of phytoplankton blooms in the N.E Atlantic (Asch *et al.*, 2019). Furthermore, long term trends already show that the N.E Atlantic has experienced major changes in phytoplankton functional diversity over the last 60 years (i.e. -5% dinoflagellates decade<sup>-1</sup> whereas diatoms increased by 0.1% decade<sup>-1</sup>) due to rapid warming and various environmental transformations attributable to climate change (Bedford *et al.*, 2020; Holland *et al.*, 2023; Mutshinda *et al.*, 2024). All of this strongly supports the pressing needs for further investigations on phytoplankton-aerosol interactions as environmental stressors will result in significant non-linear effects and tipping points (Ban *et al.*, 2022; Wolf *et al.*, 2024).

In contrast to PMOA, marine Secondary Organics Aerosols (SOA) in the remote MBL arise from new particle formation (NPF) and are governed by subtle chemical mechanisms. These include gas-to-particle conversion (Peltola *et al.*, 2022; Zheng *et al.*, 2021), oxidation of volatile organic compounds and consequent volatility reduction that leads to condensation (Kroll *et al.* 2018; Hallquist *et al.* 2009), ion-induced nucleation of biogenic particles (Kirkby *et al.*, 2016) and fission of organic biogels (Karl *et al.*, 2013). SOA formation occurs through various processes such as homogeneous, heterogeneous and multiple phase reactions (Marais *et al.*, 2016; McNeill, 2015) as well as photochemical reactions (Brüggemann *et al.* 2018). While various SOA molecular classes have been identified, the complexity of SOA, which consist of thousands of multifunctional compounds (Goldstein and Galbally, 2007) including high molecular weight species and oligomers from diverse sources underscores the pressing need for continued exploration. All of this can now be partly described thanks to



continuous widespread progresses in aerosol mass spectrometry (DeCarlo *et al.* 2006; Laskin, and Nizkorodov 2012). The present study focuses on source apportionment, aiming to delineate the sources of marine OA, particularly distinguishing between SOA and PMOA sources.

85 Both SOA and PMOA serve as cloud condensation nuclei (CCN) (Mayer *et al.*, 2020), impacting cloud albedo and lifetime, leading to uncertainties in global chemistry-climate models (Bellouin *et al.*, 2020). Radiative transfer implications from such interactions range from  $-2.65$  to  $-0.07$   $\text{Wm}^{-2}$ , contrasting with  $\text{CO}_2$  radiative forcing estimate of  $1.83 \pm 0.18$   $\text{Wm}^{-2}$  (Etminan *et al.*, 2016). In pristine environments, SOA nucleation events significantly shape CCN concentrations, altering cloud radiative forcing (Liu and Matsui, 2022) but so does the  
90 presence of primary sea spray (Fossum *et al.*, 2018). Complementing this, previous literature shows that phytoplankton activity is related to emissions of organic and sulphate particle CCN precursors (O'Dowd *et al.*, 2015; Sanchez *et al.*, 2021). There is an ongoing debate over the respective impacts from primary sea spray (Ovadnevaite *et al.* 2011; King *et al.* 2012; Schwier *et al.* 2015; Xu *et al.* 2021) and secondary aerosols (Mayer *et al.*, 2020; Quinn *et al.*, 2017) on cloud formation in pristine environments. This study, thus, aims at identifying  
95 aerosol sources and quantifying elemental ratios which can serve as a proxy for ulterior parametrisations (e.g. as done in Han *et al.* 2022; Li *et al.* 2023).

Finally, the effects from ocean biology are currently unaccounted for in climate models (Sellegrì *et al.*, 2021), therefore, this study seeks to relate different aerosol sources and geographical regions to phytoplankton taxonomic group simulations (Rousseaux *et al.* 2013). This multi-faceted approach allows to place the local  
100 measurements at Mace Head into the broader context of ocean-atmosphere interactions and explore the potential influences of marine ecosystems on atmospheric aerosol loading over the North Atlantic region.

## 2. Materials and Methods

### 2.1 Site Description

Mace Head (MHD) atmospheric research station is located on the west coast of Ireland ( $53.33^\circ\text{N}$ ,  $9.90^\circ\text{W}$ ) on a  
105 peninsula exposed to open ocean air masses. These air masses, originating from a nominal clean sector (between  $190^\circ$  and  $300^\circ$ ; Grigas *et al.* 2017) are predominantly steered by westerlies ushered by the polar jet's low-pressure systems. Importantly, open ocean air masses are mostly devoid of anthropogenic influences, with over 60% of air masses arriving at MHD classified as pristine marine (Grigas *et al.*, 2017; Sanchez *et al.*, 2022). However, the remaining 40% of all the other air masses from the 360 sector exhibit varying degrees of  
110 anthropogenic influences, particularly during or just after periods of continental outflow under high-pressure regimes (Jennings *et al.* 2003).

This study focuses on August 2015, a summertime period characterized by heightened biological activity (Behrenfeld *et al.*, 2019) and predominant pristine marine conditions. This specific year is also marked by the onset of the *cold blob*, with the subpolar gyre region (The North Atlantic waters south of Greenland) reaching  
115 around  $2^\circ\text{C}$  lower than previous long-term average possibly owing to the slowing down of the Atlantic Meridional circulation and Greenland Ice melt (Rahmstorf *et al.*, 2015; Sanders *et al.*, 2022). As such these specific conditions could serve as an indication for future measurements of aerosols-phytoplankton interactions during future cold blob phenomena.



## 2.2 In-situ measurements

- 120 Ambient submicron non-refractory aerosol major species were monitored using an Aerodyne high-resolution  
time-of-flight aerosol mass spectrometer (HR-ToF-AMS) equipped with a standard tungsten vaporizer operated  
at 650°C. The instrument working principles have been extensively described in the literature (Canagaratna et  
al., 2007; DeCarlo et al., 2006). The HR-ToF-AMS used a 5 min time resolution scan on the single-reflection  
highly sensitive V mode configuration (mass resolution up to 3000 m/Δm) while detection limits were estimated  
125 based on the approach described by Drewnick *et al* (2009). Ionisation efficiency (IE), particle velocity and inlet  
flow were determined following standard methods while applying standard RIEs (Nault et al., 2023; Xu et al.,  
2018). The particle transmission and detection efficiency expressed as the collection efficiency (CE; Huffman *et al.*  
2005) was corrected for detection losses due to particle bounce and lens efficiency by applying the  
composition-dependent collection efficiency (Middlebrook *et al.* 2012)..
- 130 The AMS data were analysed using SQUIRREL (SeQUential Igor data RetRiEvaL) v1.65B and PIKA (Peak  
Integration by Key Analysis) v1.25B software packages. Sea salt was estimated based on a scaling factor of 51  
of the common sea salt ion NaCl<sup>+</sup> (m/z 57.96) (Ovadnevaite et al. 2012) while MSA was quantified by upscaling  
the CH<sub>3</sub>SO<sub>2</sub> (m/z 79) ion (Ovadnevaite *et al.*, 2014). Interferences from MSA on SO<sub>4</sub> and OA were accounted  
for as follows:

$$135 \quad SO_{4 \text{ corrected}} = SO_4 - \frac{CH_3SO_2 * 12.48}{RIE_{SO_4}} \quad (1)$$

$$OA_{\text{corrected}} = OA - \frac{CH_3SO_2 * 15.86}{RIE_{Orgs}} \quad (2)$$

- An improved Ambient (I-A) method was adopted for the mass spectra elemental ratio analysis of O:C, H:C, N:C,  
S:C, and the OM:OC (organic matter to organic carbon) ratio (Canagaratna et al., 2015). High-resolution  
analysis was performed on each m/z in the mass range 12–130 m/z with ion fitting applied to difference between  
140 open and closed spectra. Based on their elemental composition (C, O, H, N, S), ions were then grouped into  
chemical families: C<sub>x</sub>, C<sub>x</sub>H<sub>y</sub>, C<sub>x</sub>H<sub>y</sub>O<sub>z</sub> (z = 1), C<sub>x</sub>H<sub>y</sub>O<sub>z</sub> (z > 1), C<sub>x</sub>H<sub>y</sub>N<sub>w</sub> (w = 1), C<sub>x</sub>H<sub>y</sub>N<sub>w</sub> (w > 1), C<sub>x</sub>S<sub>j</sub>, H<sub>y</sub>O<sub>z</sub>, N<sub>w</sub>H<sub>y</sub>,  
N<sub>w</sub>O<sub>z</sub>, S<sub>j</sub>O<sub>z</sub>, and C<sub>x</sub>S<sub>i</sub> where the indices x, y, z, w, j represent the number of C, H, O, N, S atoms, respectively.

- The concentration of equivalent black carbon (eBC) was measured by a multi-angle absorption photometer  
(MAAP, Thermo Fisher Scientific model 5012). The MAAP operated at a flow rate of 10 L min<sup>-1</sup> and a 5 min  
145 time resolution. The transmittance and reflectance of eBC-containing particles were measured by the MAAP at  
two different angles to derive optical absorbance as detailed in (Xu et al., 2020).

Carbon monoxide (CO) measurements were also conducted using a model RGA-3 CO analyzer (Trace  
Analytical, Inc., CA, USA), which operates on the principle of hot mercuric oxide reduction gas chromatography  
(Derwent et al. 1994).

- 150 Ozone (O<sub>3</sub>) was measured with an UV O<sub>3</sub> spectrometer (Model 8810, Monitor Labs San Diego, CA), the raw  
voltage output was converted to concentration values based on Automatic Urban/Rural Network (AURN)  
calibration audits (Derwent *et al.* 2018). Finally, meteorological data were continuously recorded at the station  
(including rainfall, solar radiation, wind speed, wind direction, temperature, relative humidity and pressure)



155 using standard meteorological instruments and retrieved using the *worldMet* R package (station ID: 039630-99999) from the NOAA ISD website (<https://www.ncdc.noaa.gov/isd>).

### 2.3 Source apportionment

The HR organic mass spectra was deconvolved using the Positive Matrix Factorization (PMF; Paatero and Tapper 1994; Paatero 1999) source-receptor model to investigate the various source contributions to OA. A major advantage of using HR data over unit mass resolution is the distinct differentiation of multiple ions sharing the same nominal mass, thereby allowing for a more exact characterisation of the temporal fluctuations of different ion families (e.g.,  $C_xH_y^+$ ,  $C_xH_yO_z^+$ ). The information richness in the HR-ToF-AMS datasets, as a result of the improved chemical resolution, is advantageous for restricting the PMF solutions, minimizing rotational ambiguity and results in more reliable solutions and a larger number of interpretable OA factors.

The IGOR PRO Source Finder (SoFi v6.8.1) toolkit (Canonaco *et al.* 2013) was used to run the PMF algorithm. Solutions were assessed across 2 to 12 factors using the unconstrained factors rotational Fpeak tool. Factors were explored for Fpeaks (rotations) between  $-1$  and  $1$  (0.1 steps). A final solution consisting of 4 factors was retained as the optimal solution based on several considerations. These include its Q/Qexp ratio value (1.38), which is tested for a range of FPEAKS and scaled residuals distribution (as recommended by Zhang *et al.* 2011). The solutions were also investigated in regard to key diagnostic plots, diurnal profiles, correlations with meaningful external tracer time series and reference mass spectra (Canonaco *et al.* 2021) extracted from the aerosol mass spectrometer database (Ulbrich *et al.*, 2009).

### 2.4 Air masses trajectory analysis

Air masses back trajectories analysis was performed using the Hybrid Single Particle Lagrangian Integrated Trajectory (HYSPLIT) (Stein *et al.*, 2015). Meteorological data were accessed from the Global Data Assimilation System (GDAS) archived by NOAA Air Resources Laboratory. HYSPLIT was used to calculate 72 hours back trajectories every 3 hours with starting height set to 100m above ground level. To investigate potential source regions leading to total particle mass concentrations from each resolved source, the back trajectories were gridded to  $1^\circ \times 1^\circ$  grid cells and linked to particle concentrations using trajectory source contribution functions. While common source contribution functions assume that trajectories centrelines are accurate, we focused instead on the Simplified Quantitative Transport Bias Analysis (STQBA) method which considers plumes transport bias along air mass trajectories as a more robust approach.

The Boundary layer height (BLH) was determined from the fifth generation ECMWF (European Centre for Medium-Range Weather Forecasts) atmospheric reanalysis (ERA5) dataset based on the bulk Richardson number (Guo *et al.*, 2021) by mapping HYSPLIT trajectories footprint along the gridded BLH data. This was used to find the fraction of time spent over the Ocean, within the Marine Boundary Layer (MBL; altitude  $<BLH$ ), in the Marine Free Troposphere (MFT; altitude  $>BLH$ ) and over land in the planetary boundary layer (PBL; altitude  $<BLH$ ). The R package *rnaturalearth* was also used to obtain a high-resolution land mask for Ireland allowing for identification of purely marine air masses (no advection over land for at least 3 days prior to being sampled at MHD) and aided in delineating lands from oceans.

190 Finally, NASA Ocean Biogeochemical Model (NOBM) taxonomic group simulations (Rousseaux *et al.*, 2013) for *coccolithophores*, *diatoms*, *chlorophytes* and *cyanobacteria* were used to visualise phytoplankton geographic repartition estimates as well as for lags calculations with OA similarly to O'Dowd *et al.* (2015).



## 2.5 Transfer entropy analysis

195 The R package *RTransferEntropy* (Behrendt et al., 2019) was used to quantify the information flow between  
time series using the transfer entropy (TE) as previously done on recent SOA studies (Long et al., 2023; Sinha et  
al., 2024). Transfer entropy (TE) is a prediction model that quantifies the directional influence between two time  
series X and Y by determining how the past values of one series predict the future behaviour of the other  
(Schreiber, 2000). TE is calculated using Rényi entropy, a generalisation of Shannon entropy that offers  
enhanced robustness in the presence of tails effects. To account for spurious information transfer, the transfer  
200 entropy is also estimated from a shuffled version of the time series. This shuffled estimate called *effective  
transfer entropy* (eTE) is used to correct for sampling bias, ensuring the validity of the results. Statistical  
significance is assessed with a bootstrapped Markov chain, where a p-value of less than 0.05 indicates a  
significant information transfer between X and Y. The reader is referred back to Behrendt et al. (2019) for more  
details.

## 205 3. Results

### 3.1 Submicron aerosol chemical composition overview

The mass concentration time series of organic aerosols (OA), methane sulphonic acid (MSA), sulfate ( $\text{SO}_4^{2-}$ ),  
nitrate ( $\text{NO}_3^-$ ), ammonium ( $\text{NH}_4^+$ ) and sea salt measured by the HR-ToF-AMS as well as eBC from MAAP  
measurements are shown on Figure 1. The average chemical composition was dominated by OA (32%),  
210 followed by  $\text{SO}_4^{2-}$  (31%), sea salt (20%), MSA (7%),  $\text{NH}_4^+$  (6%),  $\text{NO}_3^-$  (2%) and eBC (2%) (Figure 1).

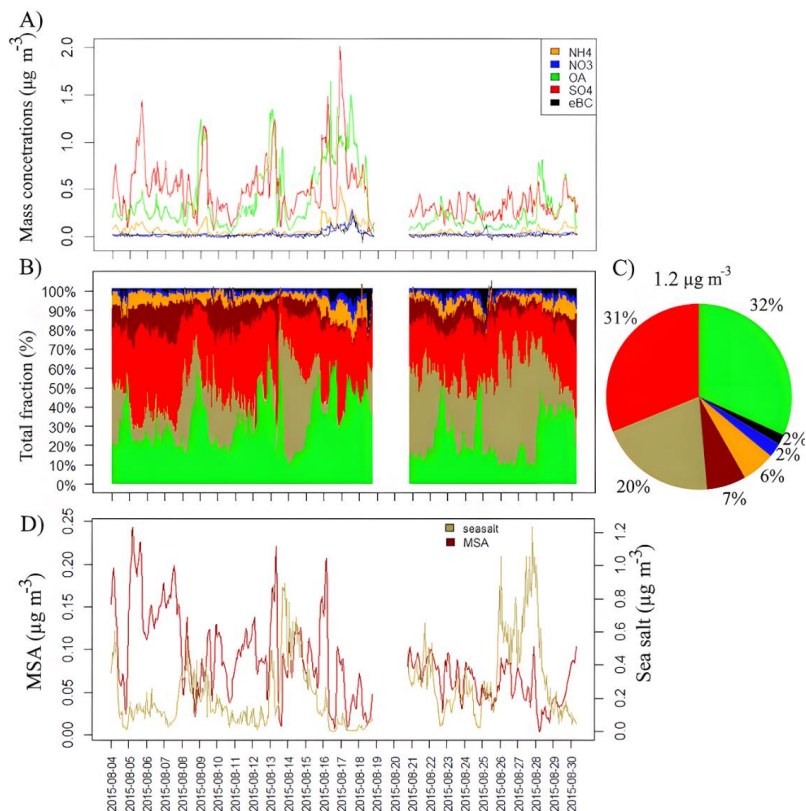




**Figure 1: A) OA, SO<sub>4</sub>, NH<sub>4</sub>, NO<sub>3</sub> and eBC mass concentrations time series –  $\mu\text{g m}^{-3}$  B) Relative contributions to total PM<sub>1</sub> C) Pie plot of total contributions to total PM<sub>1</sub> D) shows MSA and sea salt –  $\mu\text{g m}^{-3}$ .**

215 The total average bulk submicron aerosol mass was  $1.2 \mu\text{g m}^{-3}$  over the entire measurement period. These high SO<sub>4</sub><sup>2-</sup> and OA relative contributions and overall low concentrations are common for coastal sites during summertime in the marine boundary layer as reported over the North & South Atlantic Ocean (Ovadnevaite *et al.*, 2014; Huang *et al.*, 2018) as well as in the Arctic (Willis *et al.*, 2017; Nielsen *et al.*, 2019). MSA in particular showed mass concentrations values of  $0.08 \pm 0.04 \mu\text{g m}^{-3}$  in the range of those previously reported at Mace Head (0.05±0.04) (Ovadnevaite *et al.* 2011) and more diverse locations such as the central Arctic (Dada *et al.*, 2022) and the Atlantic Ocean from 53° N to 53° S where average mass concentrations of  $0.04 \pm 0.03 \mu\text{g m}^{-3}$  (Huang *et al.*, 2018) were reported.

The low mass concentrations of NH<sub>4</sub><sup>+</sup>, NO<sub>3</sub> and corresponding N:C ratio of  $0.006 \pm 0.002$  (Figure S1), indicate a limited presence of amino acids (below detection limit) from usual sources such as the North Atlantic oligotrophic gyre, ornithogenic emissions (i.e., birds), phytoplankton, bacteria, or in situ atmospheric processes (Schmale *et al.*, 2013; Van Pinxteren *et al.*, 2022).

230 Following eBC thresholds established for the North-East Atlantic (Grigas *et al.*, 2017), pristine conditions (eBC levels below  $0.015 \mu\text{g m}^{-3}$ ) were observed during 60.4% of the measurement period. Clean conditions (eBC levels between  $0.015$  and  $0.05 \mu\text{g m}^{-3}$ ) prevailed 30.5% of the time, and moderately polluted conditions (eBC levels between  $0.05$  and  $0.3 \mu\text{g m}^{-3}$ ) occurred for 9.1% of the time with a significant pollution event spanning from August 17<sup>th</sup> to 19<sup>th</sup> 2015 onwards.

Likewise, CO mixing ratios were below 100 ppb for over 70% of the time, similarly to other pristine sites (Zhao *et al.*, 2022). Winds advected through the clean sector (190-300°) for over 78% of the time. Finally mean wind speed was  $6.6 \pm 3.1 \text{ ms}^{-1}$  only being below the whitecap threshold of  $4 \text{ m s}^{-1}$  (O'Dowd *et al.*, 2014) for 23% of the time hinting at strong sea spray influences.

240 SOA influences were also consequent as revealed with the average OM/OC (organic matter to organic carbon ratio) value of  $2.10 \pm 0.14$  (Figure S1), aligning with the value of 1.9 previously reported for clean aged marine polar air masses at MHD (Ovadnevaite *et al.* 2014). Additionally, AMS derived OM/OC values in the high Arctic (Nielsen *et al.*, 2019) also fall within the range of 1.96 to 2.42 for PMOA (primary marine organic aerosols) and MO-OOA (more oxidised organic aerosols) respectively, here median OM/OC value was 2.11 with minimum and maximum OM/OC values of 1.71 and 2.42 respectively. This indicates the presence of both PMOA (i.e., saturated hydrocarbons, unsaturated hydrocarbons and cycloalkanes) as well oxygenated SOA formed with photochemical processing during long range transport (Aiken *et al.*, 2008; Simon *et al.*, 2011).

245 To get a better sense of the aerosol sources, the respective contributions of the marine boundary layer (MBL), marine free troposphere (MFT) and planetary boundary layer (PBL) are shown in Figure S2. Overall, the measurement period was dominated by marine boundary layer influences (91% of the time), with minimal marine free troposphere influences (8%) and extremely low land-influences from the planetary boundary layer (1%) further hinting at pristine marine conditions.



### 3.2 Source apportionment

250 To accurately classify and categorize the diverse sources of OA that are present at Mace Head, source apportionment was performed utilizing the Positive Matrix Factorization (PMF) method on the organic mass spectrum, which ranged from  $m/z$  12 to  $m/z$  130. The resulting chosen four-factor solution, as depicted in Figure 2 yielded a  $Q/Q_{exp}$  ratio of 1.38 and accounted for up to 90% of the total measured organic aerosol mass. Solutions with a higher number of factors introduced splitting and did not show additional emergent  
255 interpretable sources (Figure S3, Text S1).

The following four factors, namely Methane Sulphonic Acid, More Oxidised Organics, Primary Marine Organics and Peat, were determined as the optimal representation of the marine aerosol at Mace Head:

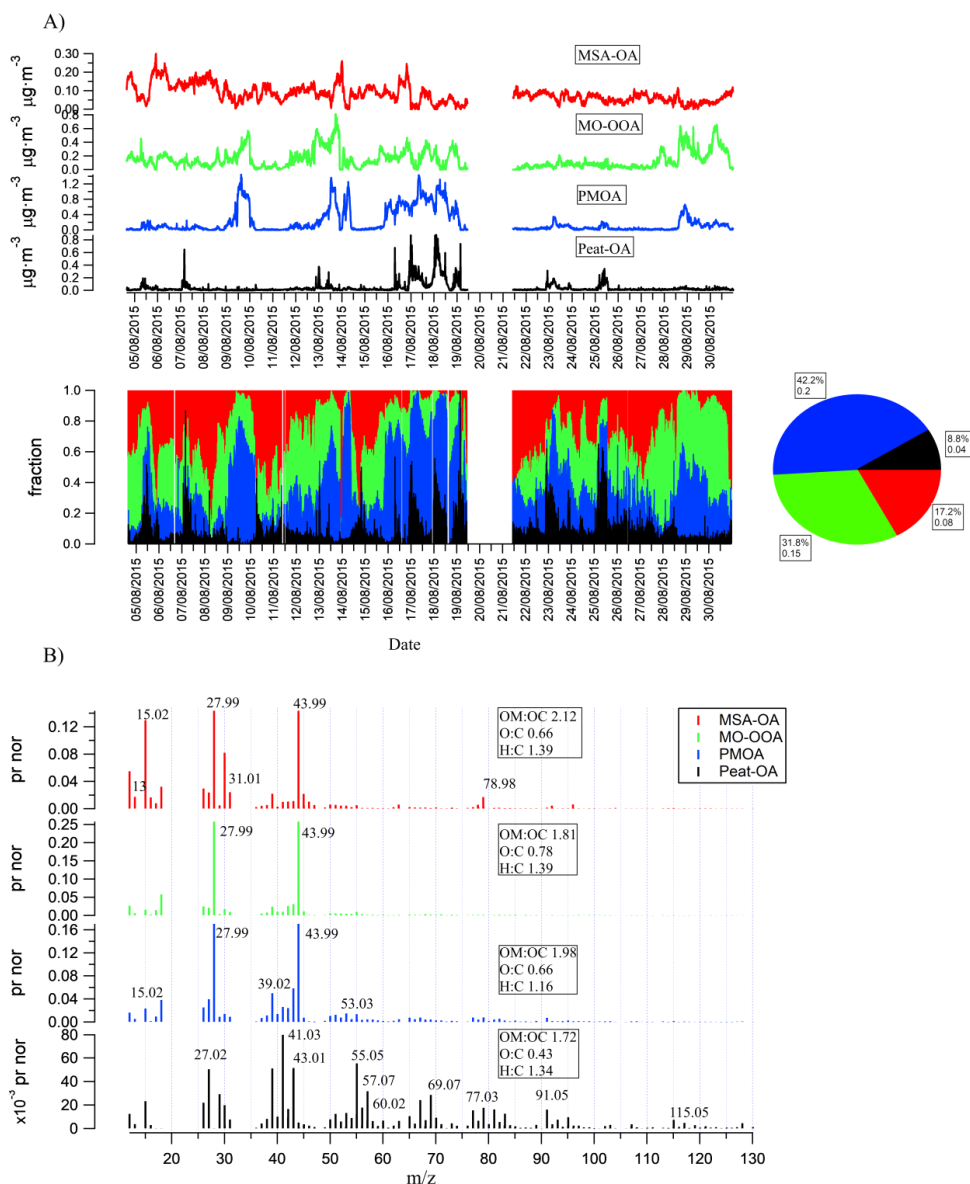
Methane Sulphonic Acid Organic Aerosols (MSA-OA): Representing approximately 17.2% of the total OA mass, MSA displayed a distinct  $m/z$  fragment at  $m/z$  78.98 ( $\text{CH}_3\text{SO}_2^+$ ), accounting for 36.3% of its total mass  
260 spectra signal intensity. The identification of specific methane sulphonic acid tracer ions further substantiated its origin. More details on all factors are provided below in sections 3.2.1-3.2.4.

More Oxidised Organic Aerosols (MO-OOA): Making up about 31.8% of the total elucidated PMF solutions, this factor exhibited prominent  $m/z$  fragments at  $m/z$  27.99 and  $m/z$  43.99 and showed significant correlations with reference mass spectra for MO-OOA ( $R = 0.97$ ) (Hu et al., 2015) and LO-OOA ( $R = 0.76$ ) (Mohr et al.,  
265 2012). O:C and H:C ratios were also in line with expected values for marine MO-OOA (Figure S4), correlations with external tracers and  $m/z$  ratios values further confirmed the MO-OOA designation.

Primary Marine Organic Aerosols (PMOA): Comprising roughly 42.2% of the total resolved PMF solutions. This factor exhibited  $m/z$  fragments similar to MO-OOA (Schmale et al., 2013), but with higher contributions from aliphatics ( $\text{C}_x\text{H}_y$ ) such as alkyls (dominant in sea spray during phytoplankton blooms; Cavalli et al. 2004),  
270 alkenes (i.e. phenols or humic materials; Bahadur et al. 2010) and functional derivatives such as alcohols ( $\text{C}_x\text{H}_y\text{O}_z$ , where  $z=1$ ) as established in earlier studies (Ovadnevaite et al. 2011; Crippa et al. 2013).

Peat-OA: accounting for approximately 8.8% of the total PMF solutions, was characterised by saturated hydrocarbons ( $\text{C}_x\text{H}_{2y+1}$ ), unsaturated hydrocarbons ( $\text{C}_x\text{H}_{2y-1}$ ) and cycloalkanes ( $\text{C}_x\text{H}_{2y}$ ) ion series. This factor was identified as Peat-OA owing to its good correlation ( $R=0.75$ ) with the Peat-OA reference mass spectra (Lin  
275 et al., 2017). Additionally, its mass spectrum was marked by cellulose ( $\text{C}_2\text{H}_4\text{O}_2^+$ ) at  $m/z$  60 and by the dominance of  $\text{C}_3\text{H}_7^+$  rather than  $\text{C}_2\text{H}_3\text{O}^+$  at  $m/z$  43 which facilitated the distinction of peat emissions over wood or smoky coal emissions.





280 **Figure 2. A) Factors time series (MSA-OA in red, MO-OOA in green, PMOA in blue, Peat-OA in black) and associated relative contribution time series and pie chart showing fractions and respective mass concentrations ( $\mu\text{g m}^{-3}$ ) for the whole period B) Factors mass spectra (MSA-OA in red, MO-OOA in green, PMOA in blue, Peat-OA in black) and associated improved ambient OM:OC, O:C and H:C ratios (Canagaratna et al., 2015).**



### 3.2.1 More Oxidised Oxygenated Organic Aerosols (MO-OOA)

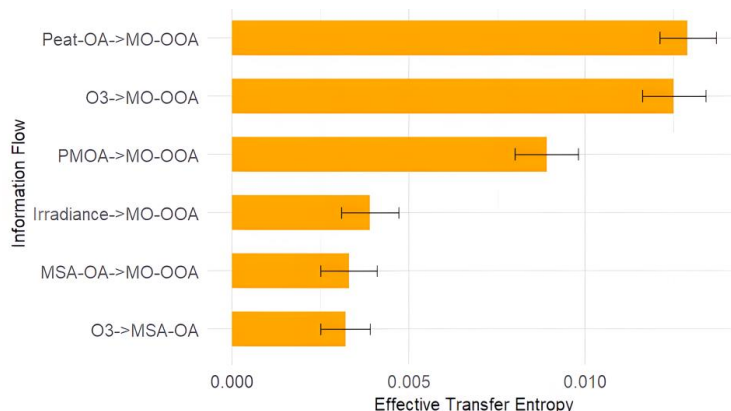
285 MO-OOA main contributing ions are associated with oxygenated compounds belonging to the COOH functional group (Figure S5), reflecting pronounced fragmentation of mono- and dicarboxylic acids into fragments with multiple oxygen atoms (Duplissy *et al.*, 2011). Specifically,  $C_xH_yO_z$  ( $z > 1$ ) ions family accounts for 63.1% of the total mass spectra intensity, followed by  $C_xH_yO_z$  ( $z = 1$ ) ions family ( $m/z$  27.99,  $m/z$  43.02,  $m/z$  42.01...) contributing 13.7% to MO-OOA, adding up to a total contribution of 76.8%. Additionally,  $CO^+$  and  $CO_2^+$  each accounts for 25% of MO-OOA intensity which is typical for remote ocean carboxylic acids (Dominutti *et al.*, 2022).

In contrast,  $C_xH_y$  (aliphatics) ions family ( $m/z$  13.00,  $m/z$  15.02,  $m/z$  16.03...) contributes only 13.7% to MO-OOA total mass spectra intensity. Nitrogen-containing ions fragments constituted a very low portion of the signal (0.8%), similarly to previous remote ocean measurements (Ovadnevaite *et al.* 2011). The weak contribution from  $C_2H_3O^+$  (3.2%) which has been reported to be predominantly due to non-acid oxygenates (Ng *et al.*, 2011a) suggests a considerable prevalence of aging/oxidation during transport over the North-East Atlantic Ocean. This is also further confirmed by the low  $m/z$  43:44 ratio of 0.12 hinting to MO-OOA rather than less oxidised species (Ng *et al.*, 2011). This factor respective O:C ratio and H:C ratio of 0.78 and 1.17 further agree with MO-OOA reported at other similar locations (Figure S4). MO-OOA also has a strong contribution from  $CO_2^+$  (25.7%) which is assumed to originate mainly from acids or acid-derived compounds (Duplissy *et al.*, 2011; Ng *et al.*, 2011) that are known to be mostly water-soluble (Decesari *et al.*, 2007) such as organic acids (e.g., mesotartaric acid, meso-erythritol, tartaric acid, oxalic acid) formed from oligomerization of small  $\alpha$ -dicarbonyls (e.g., glyoxal) (Cui *et al.*, 2022).

MO-OOA formation through ozonolysis is postulated based on a robust hourly averaged correlation ( $R=0.67$ ) of MO-OOA to  $O_3$  across the entire observational period (Figure S6-B). Using the effective transfer entropy test (Behrendt *et al.*, 2019) further reveals the non-linear dynamics between  $O_3$  and MO-OOA, indicating  $O_3$  as a significant reactant in the formation of MO-OOA from its precursors with a transfer entropy value of 0.014 (Figure 3) and an effective transfer entropy value of  $0.0127 \pm 0.0009$  ( $p$ -value $<0.05$ ). In other words, there is a significant directional information flow between the two time series. Figure 3 also shows that MO-OOA is a mix of local (Peat-OA) and regional marine influence (PMOA, but also MSA-OA to a lesser extent) all eventually concurring to MO-OOA formation, with ozone contributing 3x more information to MO-OOA than irradiance does. This aligns with studies showing  $O_3$  to be a strong oxidation driver during summertime in the marine environment (Ovadnevaite *et al.*, 2011), where unsaturated aliphatic chains (C=C double bonds) react with



ozone to form oxidised compounds (Decesari *et al.*, 2011).



315

**Figure 3. Significant ( $p$ -value<0.05) effective transfer entropy flow values between PMF factors, ozone and irradiance.**

### 3.2.2 Methanesulphonic Acid Organic Aerosols (MSA-OA)

The mass profile of MSA-OA reveals that two oxygenated carbon families CHO (sum of  $C_xH_yO_k$  and  $C_xH_yO_w$  where  $k = 1$  and  $w > 1$ ) dominate 53.4% of the total mass spectra fraction followed by aliphatics (pure Hydrocarbon-like,  $C_xH_y^+$ ) whose fraction accounts for 33.3% (Figure S5). MSA-OA is clearly identified owing to its substantial contribution from the  $C_xS_y^+$  family (6%) over other sources, this is in line with the  $C_xS_y^+$  contribution (7%) for MSA-OA also reported by Huang *et al.* (2018). The excellent correlation ( $R=0.82$ ) between this factor and the  $C_xS_y^+$  family (Figure S6-D) also further highlights the organosulphurs nature of MSA-OA as opposed to other factors.

325

Similarly, to results reported by Schmale *et al.* (2013), the correlation coefficient with the AMS database MSA-OA laboratory reference spectrum (Figure S6-A) is rather moderate ( $R=0.55$ ), although this factor spectra still allows for the precise identification of characteristic MSA ions at  $m/z$  44.98 ( $CHS^+$ ), 47.00 ( $CH_3S^+$ ), 64.97 ( $HSO_2^+$ ), 77.98 ( $CH_2SO_2^+$ ), 77.99 ( $CH_3SO_2^+$ ), and 95.99 ( $CH_4SO_3^+$ ). MSA-OA O:C and H:C ratios were 0.66 and 1.39 respectively, close to values (O:C: 0.54, H:C: 1.42) reported by Loh *et al.* (2022).

330

MSA-OA  $C_xH_y$  family also features a typical  $CH_3^+$  ion at  $m/z$  15.02 that is absent from other factors. Similarly, the  $C_xH_yO_w$  ( $w=1$ ) family features the tracers ions  $CH_2O^+$  (8.2%) and  $CH_3O^+$  (2.4%) which are heat stress related markers (Faiola *et al.* 2015) attributed to methyl jasmonate (MeJA) and possibly acrylic acid (Van Alstyne and Houser, 2003) or other oxylipins stress enzymes (Aguilera *et al.*, 2022; Koteska *et al.*, 2022) which are known to be emitted by kelp (Saha and Fink, 2022) or phytoplankton species (Koteska *et al.*, 2022).

335

The  $C_xS_y^+$  fragment family was dominated by  $CHS^+$  (25.9%),  $CH_3SO_2^+$  (20.2%),  $CH_2S^+$  (12.2%),  $CH_4SO_3^+$  (7.5%),  $CH_3SO^+$  (7.2%),  $CH_2SO_2^+$  (6.9%),  $CH_4SO_2^+$  (5.45),  $CH_3S^+$  (6.4%),  $C_2H_4SO_2$  (5.4%) and  $CH_2SO^+$  (2.5%) which are common MSA ions found in the literature (Moschos *et al.*, 2022). Overall, the  $C_xH_y^+$  and  $C_xS_y^+$  fragment ions families indicate a clear MSA fragmentation pattern with a characteristic high  $CH_3^+$  relative intensity (13%) typical for marine SOA in line with recent findings (Huang *et al.*, 2018; Moschos *et al.*, 2022).

340



Finally, MSA-OA correlated moderately (Figure S6-B) with particulate sulphate ( $R=0.51$ ) which is expected since dimethyl sulphide, released by phytoplankton, can be oxidized to either form MSA or sulphur dioxide and then to sulphuric acid, leading to their partitioning into the particulate phase (Mungall *et al.*, 2018).

### 3.2.3 Primary Marine Organic Aerosols (PMOA)

345 High-resolution mass spectrum of this factor reveals that two CHO oxygenated carbon families (sum of  $C_xH_yO_k$   
and  $C_xH_yO_w$  where  $x = 1$  and  $w > 1$ ) dominate 61.5% of the total mass spectra followed by aliphatics (pure  
Hydrocarbon-like,  $C_xH_y$ ) whose fraction accounts for 36.2% of the total mass spectra signal (Figure S5) aligning  
with previous findings reported by Ovadnevaite *et al.* (2011). The  $C_xH_yO_w$  ( $w=1$ ) family features ions series ( $m/z$   
55.02, 69.03, 83.05, etc...) related to alkenyl groups, diunsaturates, cyclic alcohols, and ethers. Such functional  
350 groups repartition is consistent with previous reports of water-insoluble organics being formed in sea spray  
(O'Dowd *et al.* 2004; Ovadnevaite *et al.* 2011). Additionally, this factor mass spectrum closely resembles  
( $R=0.99$ ) marine organic aerosols (MOA) mass spectra (Ovadnevaite *et al.* 2011) (Figure S6-A) and its O:C ratio  
of 0.66 and an H:C ratio of 1.16 respectively are close to literature O:C values for sea spray (Ovadnevaite *et al.*  
2011; Flerus *et al.* 2012; Willoughby *et al.* 2016) (Figure S4).

355 PMOA  $C_xH_y$  mass spectra family is dominated by ion series  $C_xH_{2y-3}$  ( $m/z$  39.02, 53.03, 67.05 etc...) indicating  
dienes, alkynes, and cycloalkenes contributions, which is further confirmed by the presence of  $C_xH_{2y-1}$  ions series  
( $m/z$  27.02, 41.04, 55.05 etc...) while the  $C_xH_{2y+1}$  family ( $m/z$  43.05, 57.07, 83.08 etc...  $y>2$ ) indicative for  
anthropogenically influenced refined hydrocarbons is absent from this factor mass spectra. The marine biogenic  
origin of this factor is also indicated by the absence of alkanes ( $C_xH_{y+2}$ ;  $m/z$  16.03, 58.08, 72.09) which are  
360 typical for continental air masses (Lewis *et al.*, 2021) and by its lack of correlation with eBC ( $R=0.17$ ) thereby  
excluding contribution from fossil hydrocarbons to PMOA. The  $C_xH_y$  family is also marked by alkyls ( $C_xH_{2y+1}$   
; $m/z$  15.02, 29.03, 37.00 etc...) which have been reported to be dominant in sea spray during phytoplankton  
blooms as a possible result of phosphate cycling (Cavalli, 2004; Meador *et al.*, 2017).

Prior atmospheric measurements have shown that PMOA containing a large fraction of alkenes and oxygenated  
365 functional groups (ie. alcohols, ethers, aldehydes, ketones) are dominated by insoluble organic colloids and  
aggregates (Facchini *et al.*, 2008; Rinaldi *et al.*, 2020) composed of microgels derived from phytoplankton  
extracellular metabolic extraction and adsorption organic pool rather than exopolymers produced from bacteria,  
with abacterial microgels aerosols being quite common and possibly accounting for 50-90% of phytoplankton  
derived organics (Bigg and Leck 2008; Bates *et al.* 2012; Liu *et al.* 2023). These bacterial exopolymers would  
370 follow the makeup of ordinary bacterial cell fragments, which comprise approximately 55% nitrogen-containing  
organics and 10% carbohydrates (Schmale *et al.*, 2013). The latter are accounted for by summing up pure  
carbohydrates (i.e.; glucose, saccharose, mannitol and glycogen) identified by typical fragments (Schmale *et al.*,  
2013; Schneider *et al.*, 2011) at  $m/z$  56.03 ( $C_3H_4O^+$ ),  $m/z$  60.02 ( $C_2H_4O^+$ ),  $m/z$  61.03 ( $C_2H_5O^+$ ) and  $m/z$  85.03  
( $C_4H_5O^+$ ) only amounting for about 1.3% of the total PMOA aerosols mass. Similarly, contributions from other  
375 bacterial tracers such as glycogen;  $m/z$  55.01 (1.4%), mannitol;  $m/z$  56.02 (0.4%) and polysaccharide species;  
 $m/z$  97.02 ( $C_5H_5O_2^+$ ) and  $m/z$  125.02 ( $C_6H_5O_3^+$ ) (Glicker *et al.*, 2022) tracer ions were also relatively poor  
(0.7%). All of this paired with below detection limit amino acids thus implicates that PMOA organic pool was  
largely shaped by abacterial processes. However, bacterial influence cannot be ruled out entirely as



380 carbohydrates might have been processed by enzymes or acidity during air masses transport and subsequent aging (Zeppenfeld et al., 2023).

### 3.2.4 Peat Related Organic Aerosols (Peat-OA)

Although the measurement period is largely dominated by pristine ocean air masses, some residential heating influence is still observed owing to local peat burning. Peat-OA (Figure S5) mass spectrum is largely dominated by  $C_xH_y^+$  ions (76.9%) such as alkyls- $C_xH_{2y+1}^+$  ( $C_4H_7^+$  at  $m/z$  55.05,  $C_2H_5^+$  at  $m/z$  29.03,  $C_3H_7^+$  at  $m/z$  43.05...),  
385 alkenes- $C_xH_{2y-1}^+$  ( $C_3H_5^+$  at  $m/z$  41.03,  $C_2H_3^+$  at  $m/z$  27.02,  $C_5H_7^+$  at  $m/z$  67.05...) and cycloalkanes- $C_xH_{2y}^+$  (possibly  $C_3H_3^+$  at  $m/z$  39.02,  $C_7H_7^+$  at  $m/z$  91.05). This factor mass spectrum correlates well ( $R=0.86$ ) with previous measurements of Peat-OA in Galway city (Lin et al., 2017) (Figure S6-A). More specifically, the presence of aromatic ion series at  $m/z$  77.03 ( $C_6H_5^+$ ) and  $m/z$  91.05 ( $C_7H_7^+$ ) (Cubison et al., 2011) and the ratio between  $m/z$  55.05 ( $C_4H_7^+$ ) and  $m/z$  57.07 ( $C_4H_9^+$ ) of 1.74 as well as the ratio between  $m/z$  43.05 ( $C_3H_7^+$ ) and  
390  $m/z$  44.01 ( $C_2H_3O^+$ ) of 1.03 all allow for the clear distinction of peat burning over other sources (Lin et al., 2017). Peat-OA was freshly emitted as evidence by the pollution wind rose (Figure S7-E, S7- F) and concurrent increase along with eBC ( $R=0.72$ ) indicating that both were locally co-emitted within the planetary boundary layer (PBL).

### 395 3.3 Elemental ratios -Van Krevelen diagram

The Van Krevelen (VK) diagram (Heald et al., 2010) provides valuable information on chemical evolution of OA as demonstrated by subsequent marine aerosols studies (Ovadnevaite et al. 2014; Willis et al. 2017; Dada et al. 2022). The VK plot of the PMF factors identified in this study superimposed with bulk OA O:C and H:C values is depicted in Figure 4. Overall, the bulk OA slope of -1.18 and  $\overline{Osc}$  values spanning over -1.8 to 0.8 in  
400 the carbon oxidation state space indicates that higher levels of oxidation involving the generation of carboxylic acids, and the subsequent breakdown of the carbon backbone are prevalent over the measurement period which is consistent with MO-OOA functional groups (Heald et al.2010, Ng et al., 2011). The O:C ratios for MO-OOA, PMOA and MSA-OA all fall within the range of 0.64–1.15 reported for diverse OOA factors from previous studies (Aiken et al., 2008; Jimenez et al., 2009). All PMF factors have H:C values lower than 2 which indicate  
405 that they all contain unsaturated carbons capable of reacting with  $O_3$  (Ovadnevaite et al. 2011). This is evidenced by effective transfer entropy flow analysis (Behrendt et al., 2019) between Peat-OA, PMOA, MO-OOA, MSA-OA and  $O_3$  values (Figure 4) which indicates that Peat-OA had the highest information transfer flow, making it the most susceptible to ozonolysis, closely followed by PMOA and, to a lesser extent, MSA-OA. Both Peat-OA (O:C=0.43, H:C=1.34) and PMOA (O:C=0.66, H:C=1.16) VK positions broadly fall in the area consistent with  
410 lignin-like compounds (H/C = 0.6–1.5, O/C = 0.1–0.6; Park et al. 2022) which have been largely associated with terrestrial origin OA (Jang et al., 2022) and found to be high in Arctic Ocean air masses as well (Choi et al., 2019) with authors reporting ~30% of the total assigned molecular formulae as marine lignin-like compounds. These lignin-like compounds are also know to oxidise and form Humic-like molecules, characterized by polar carbonyl (keto and carboxyl) functional groups alongside hydrophobic aliphatic chains (Cavalli, 2004) which  
415 broadly agrees with MO-OOA functional groups.

MSA-OA (O:C=0.66, H:C=1.9) is then also examined by colouring the VK scatter plot (Figure S8) with the MSA-OA/ $SO_4$  ratio, a proxy for biological marine sources contributions from DMS (Chen et al., 2021) with

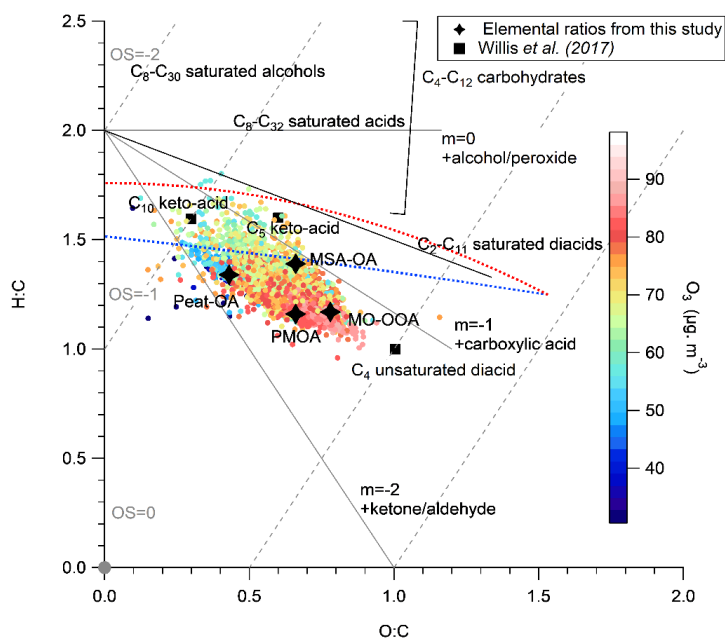


values ranging from 0.001 (ubiquitous anthropogenic influences) to 0.354 (significant contribution from biological marine sources) with an average value of 0.102 in line with pristine conditions (Huang *et al.*, 2018).

420 Figure S8 shows that high MSA-to-sulphate ratio were consistent with VK regions for C<sub>2</sub>-C<sub>12</sub> saturated diacids and inconsistent with C<sub>4</sub>-C<sub>12</sub> carbohydrates (trehalose, erythritol, arabinol, mannitol, sucrose, galactose, glucose, fructose etc...) similarly to results reported for summertime Arctic aerosols (Wilis *et al.*, 2017). However, as opposed to Arctic aerosols, H:C ratios being higher, we report no association with VK areas for C<sub>4</sub> unsaturated diacids (e.g maleic and fumaric acid) nor with C<sub>10</sub> and C<sub>5</sub> keto-acids (levulinic and pinonic acid) which are

425 aqueous photochemistry tracers from isoprene and  $\alpha$ -pinene oxidation (Kołodziejczyk *et al.*, 2019; Rapf *et al.*, 2017). This is in line with the absence of other isoprene tracers; C<sub>4</sub>H<sub>5</sub><sup>+</sup> (0.5%) at m/z 53.03 and C<sub>5</sub>H<sub>6</sub>O<sup>+</sup> (0.2%) at m/z 82.04 (Hu *et al.*, 2015; Robinson *et al.*, 2011) and monoterpene tracers (Boyd *et al.*, 2015), namely C<sub>5</sub>H<sub>7</sub><sup>+</sup> at m/z 67.05 (0.1%) and (C<sub>7</sub>H<sub>7</sub><sup>+</sup>) at 91.05 (0.1%). This is also supported with the lack of covariance (Cov[X, Y]  $\approx$  0) between bulk CO<sub>2</sub><sup>+</sup>, CO<sup>+</sup> and C<sub>2</sub>H<sub>3</sub>O<sup>+</sup> time series which also denotes the absence of non-acid

430 carbonyls (naCO) (Yazdani *et al.*, 2022) which are known to be derived from isoprene and monoterpenes (Russell *et al.* 2011). The reasons behind the absence of isoprene and monoterpenes influence on OA in these findings are currently unclear although processes such as surface ocean consumption or unexplored oxidations pathways could be a possibility (Benavent *et al.*, 2022).



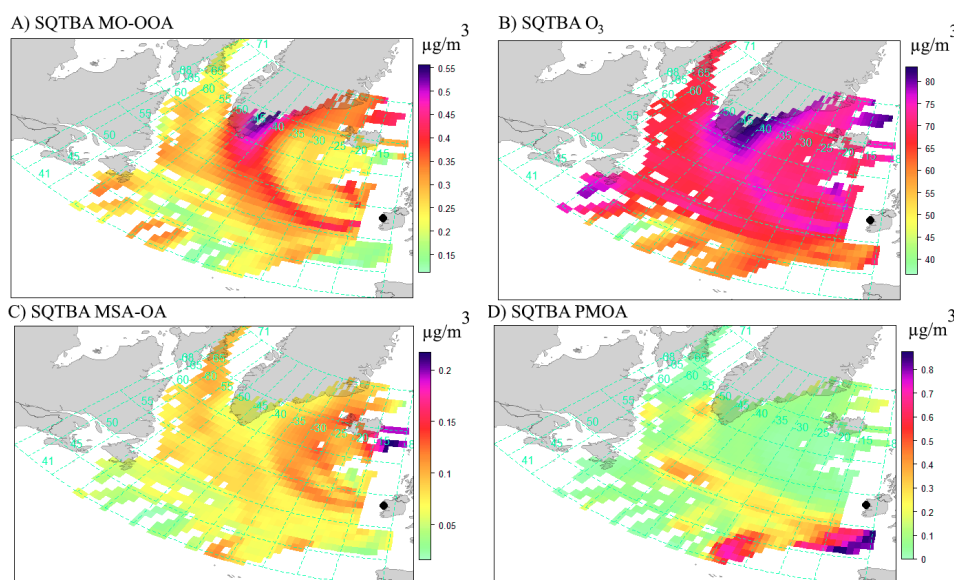
435 **Figure 4. Relationship between the ToF-AMS estimated hydrogen-to-carbon (H/C) and oxygen-to-carbon (O/C) ratios of organic species [Canagaratna *et al.*, 2015] coloured by O<sub>3</sub> mixing ratio, all observations above ToF-AMS detection limits are shown for the entire period. Grey lines represent the ambient range of O/C and H/C observed by Ng *et al.* [2011] while dashed line represent the average carbon oxidation state (OS  $\approx 2 \times O : C - H : C$ ) (2011) superimposed on the Van Krevelen diagram (Ng *et al.* 2011, Kroll *et al.*, 2011).**

440 **Elemental composition of C<sub>8</sub>-C<sub>30</sub> saturated alcohols, C<sub>8</sub>-C<sub>32</sub> saturated acids, C<sub>2</sub>-C<sub>11</sub> saturated diacids,**



C4 unsaturated diacid (maleic and fumaric acid), C4 –C12 carbohydrates (e.g., trehalose, erythritol, arabinol, mannitol, sucrose, galactose, glucose, and fructose), and C5 and C10 ketoacids (levulinic and pinonic acid, respectively) are shown for reference (Willis *et al.*, 2017).

### 3.4 Air masses and source apportionment

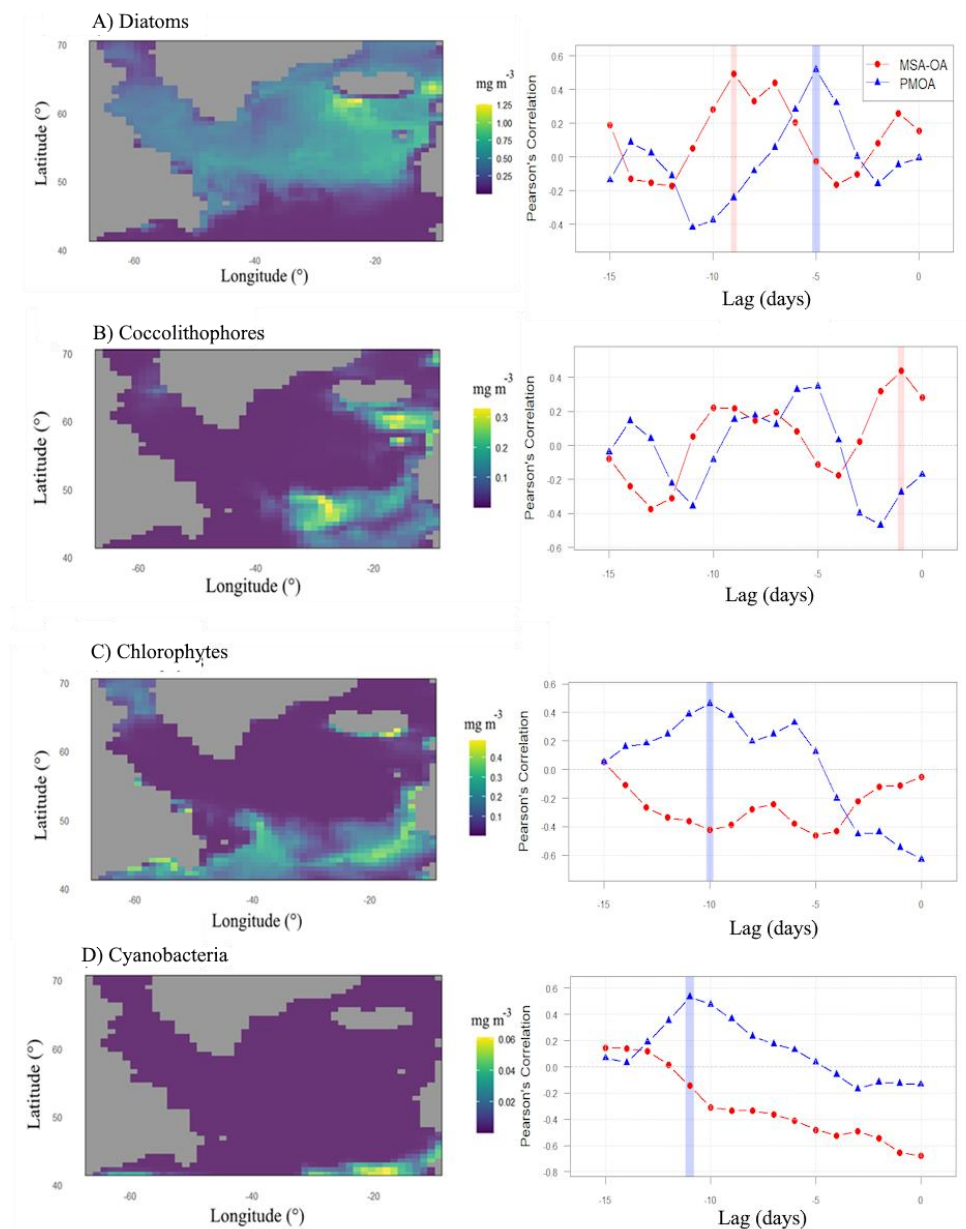


445

**Figure 5. Simplified Quantitative Transport Bias Analysis (SQTBA) -Gaussian Air masses dispersion for PMF sources (PMOA, MO-OOA, MSA-OA) and O<sub>3</sub>.**

MO-OOA (Figure 5-A) strongest sources can be traced back northward along a cyclonic gradual crescent shape spreading from Greenland Seas South of Cape Farewell (See Figure S9 for Ocean areas toponomy). This culminates further with air masses origins spanning over the East Greenland Current (Denmark Strait) upwards to the Iceland Sea south of Jan Mayen. MO-OOA is otherwise ubiquitous and shows contributions over the Newfoundland, Labrador and Iceland basins as well as other areas. O<sub>3</sub> (Figure 5-B) shared similar origin as MO-OOA further confirming its role in MO-OOA formation. Overall, we observe aged polar air masses eventually flowing from Greenland to MHD. The sustained blockade and aging of air masses over Greenland is known and attributed to summertime high-pressure systems surrounding this region influenced by Arctic amplification (Pettersen *et al.*, 2022; Preece *et al.*, 2023) where Irminger current also acts as a hotspot for turbulent eddies and heat transport which might contribute to aerosol nucleation (Semper *et al.*, 2022). Here the presence of a blocking anticyclone transition (Figure S10) leading to reduced cloud cover and warm air advection might ultimately have contributed to an increase in aged SOA at the southern tip of Greenland possibly owing to its orography.

450  
455  
460



465 **Figure 6.** Time averaged maps (0.67 x 1.25 deg) over 2015-Aug, Region 59W, 37N, 34E, 82N of dominant  
phytoplankton groups from NOBM Model data (Rousseaux *et al.* 2017; Buchard *et al.* 2017) and  
corresponding lagged cross correlations for MSA-OA (red) and PMOA (blue) against A) Diatoms B)  
Coccolithophores, C) Chlorophytes and D) Cyanobacteria :blue and red shaded areas correspond to  
maximum significant cross-correlations extracted from the autocorrelation function (ACF) 95%  
470 criteria.

470





MSA-OA (Figure 5-C) main sources include the Iceland basin and more specifically the Iceland-Faroe Ridge. This is consistent with literature highlighting the diversity of eukaryotic phytoplankton in the Icelandic marine environment with the haptophyte coccolithophore *Emiliana huxleyi* being dominant during summertime (Cerfonteyn et al., 2023) owing to nutrients transport by the North Atlantic Current acceleration (Oziel et al., 2020) and findings (O'Dowd et al. 2015; Mansour et al. 2023) indicating concomitant MSA concentrations uptick during summertime. MSA-OA also spans along the East Greenland Current (Denmark Strait) where wind-driven coastal upwelling (Håvik and Våge, 2018) might result in increased DMS emissions (Edtbauer et al., 2020). Likewise, MSA-OA extend moderately over diverse regions such as the North-Western European Basin, the Newfoundland basin (where intense DMS fluxes have been reported; Bell et al. 2021) and the Labrador Sea.

PMOA (Figure 5-D) on the other hand strongly extends over the South of the Celtic Sea and West of the Bay of Biscay as well as West European basin waters and are otherwise diffused all over the North Atlantic Ocean with moderate intensity hotspots over the Newfoundland basin (Davis strait) possibly owing to an inflated subpolar gyre (Hátún et al., 2016).

Examination of NOBM model data (Figure 6) further reveals distinct MSA-OA and PMOA patterns. MSA-OA overlap with coccolithophores dominated ecoregions as well as diatoms ones. Similarly, diatoms also seem to contribute to PMOA sources, which is in line with recent results hypothesising that diatoms have a greater atmospheric significance than other eukaryotes due to their observed enrichment in PMOA (Alsante et al., 2021) whereas association with coccolithophores appears much weaker than for MSA-OA. Another distinction lies in PMOA overlapping with chlorophytes (*flagellates*, *Phaeocystis spp*) over the Western European basin. This geographic area hosts more than 512 chlorophyte species (Narayanaswamy et al., 2010) with recent reports of chlorophytes being one of the key contributors to marine productivity (Landwehr et al., 2021), further research is warranted to fully understand their role along other phytoplankton in this region during summertime. Likewise, cyanobacteria (combination of *Synechococcus*, *Prochlorococcus*, and nitrogen fixers such as *Trichodesmium*) might also contribute to PMOA more sparsely, especially at lower latitudes in the North Atlantic Ocean as previously reported (Baer et al., 2017).

Calculated lagged correlations (Figure 6) further pointed at MSA-OA being directly associated with coccolithophores (with a lag of -1 day) as well as diatoms (lag of -9 days), however no significant correlations were observed for either cyanobacteria or chlorophytes. As opposed to MSA-OA, the association between coccolithophores and PMOA doesn't appear as meaningful (their autocorrelations are not statistically significantly different from zero). PMOA on the other hand are also associated with diatoms (lag of -5 days) and show unique associations with chlorophytes (lag of -10 days) as well as cyanobacteria (lag of -11 days).

Overall, association between OA enriched sea spray time series and phytoplankton groups remains controversial owing to a wide range of governing mechanisms as highlighted by previous studies using chl- $\alpha$  as a proxy to calculate cross correlation time lags over the North Atlantic which were found to vary between 8 days (Rinaldi et al., 2013) and 24 days (O'Dowd et al., 2015) depending on the period and length of measurements.

Late summer measurements (Mansour et al., 2020) show partially comparable lags to this study with a reported oceanic biological activity affecting aerosol properties within the order of 10-20 days. This delay roughly spans



over the full blooming to decaying phase transitions of an algal bloom (Lehahn et al., 2014) and is linked to the  
510 release of SSA-transferable organic matter in surface seawater by the interaction with marine viruses causing the  
demise of phytoplankton blooms (O'Dowd et al., 2015).

Here, by focusing on the lagged correlations between PMF factors and specific phytoplankton groups rather than  
bulk-OA and chl- $\alpha$ , this study's findings indicate that PMOA is formed on such timescale from cyanobacteria  
and chlorophytes (lags of -11 and -10 days respectively) owing to atmospheric transport from the Western  
515 European basin whereas overwhelming diatoms influence results in a much shorter lag of -5 days. Additionally,  
MSA-OA is rapidly produced from coccolithophores blooms in 1-2 days. This reflects stressed, senescent,  
grazed, or virus-infected phytoplankton releasing high quantities of DMSP which rapidly oxidises to form MSA-  
OA (Mansour et al., 2020).

Finally, the interpretation of diatoms' role on either MSA-OA or PMOA remains ambiguous as the -5 days lag  
520 with PMOA could hint at lipase activity concurring to self-aggregation and formation of free fatty acids during  
bloom potentially followed by a post-bloom (lag of -9 days with MSA-OA) with significantly different taxa or  
simply advection from remote eco-regions further closer to the Arctic which have been reported to host rich  
MSA producing diatoms communities as opposed to more southerly latitudes (Becagli et al., 2016).

#### 4. Conclusions

525 This study leverages high-resolution online aerosol mass spectrometry source apportionment to investigate the  
chemical composition and sources of submicron organic aerosols representing marine environment during a  
summertime period marked by phytoplankton blooms. The results emphasise balanced mass contributions from  
POA (PMOA and Peat-OA) and SOA (MO-OOA and MSA-OA), each category accounting for approximately  
50% of the total submicron organic aerosol mass, with distinct chemical compositions reflective of their varied  
530 origins.

One of this study's key finding is that summertime polar air masses undergo significant ozonolysis over the  
remote ocean which happens to be largely driven by Greenland blocking air masses aging and anticyclonic  
conditions. Transfer entropy is introduced here to explain the dynamics of ozonolysis in this context revealing  
significant information transfer to MO-OOA during unsaturated aliphatic chains (C=C double bonds) breakdown  
535 of PMOA as well as MSA-OA to a lesser extent. However, this transfer entropy approach additionally shows  
that MO-OOA is also being formed locally from Peat-OA oxidation, as such, further studies will aim at exactly  
delineating open ocean versus locally produced MO-OOA.

Another essential takeaway is that OA not only reflect atmospheric chemistry and meteorology but may also  
serve as an indicator of marine ecosystems (i.e. MSA-OA enzymes stress makers and PMOA phytoplankton  
540 extracellular metabolic processes markers). Air masses trajectory analysis also show aerosols-phytoplankton  
ecoregions contributions with MSA-OA traced to the Iceland Basin and the Iceland-Faroe Ridge, with a rapid  
production burst (lag of 1-2 days) following coccolithophore blooms. Whereas relationship with diatoms show  
much longer lag (9 days) indicating fundamentally different oceanic biological processes. In contrast, PMOA is  
sourced from more diverse ecoregions (Southern Celtic Sea, West European Basin, and Newfoundland Basin),  
545 with additional chlorophytes and cyanobacteria influences from more southerly latitudes. All of this suggests  
that different phytoplankton taxa contributions to OA lead to specific m/z tracers and functional groups



repartition (i.e. sulphides as coccolithophores tracers, aliphatics as tracers for diatoms) though further investigation is needed to explore the biological processes and ecoregions specificities influencing this relationship. Overall, this study demonstrates the complex aerosol chemistry and diverse geographic origins  
550 influencing POA and SOA formation in the Northeast Atlantic marine environment. Our findings emphasise the need for further long-term investigation to fully account for the various precursors and pathways contributing to OA, given their significant impacts on aerosol-climate interactions.

*Author contribution.* JO, COD and DC designed the research. DC, JO and KNF operated the instruments and verified the raw data. EC and JO produced the postprocessed data and figures. JO, COD, LL, DC, WX and LC re-edited the manuscript. EC wrote the paper with support from all authors who commented on the paper.  
555

*Competing interests.* The authors declare that they have no conflict of interest.

*Acknowledgments.* This work was supported by the EPA-Ireland and Department of the Environment, Climate and Communications and University of Galway College of Science and Engineering Postgraduate Fellowship n°127407. C. Lin acknowledges the support from the International Partnership Program of the Chinese Academy of Sciences (Grant No. 175GJHZ2022039FN). The authors would also like to acknowledge the support from the SFI FFP award (22/FFP-A/10611) and from the EPA-Ireland AC<sup>3</sup> network. Finally, we would also like to extend our gratitude to Seraphine Hausser for looking into geopotential height anomalies and producing figure S10.  
560  
565

*Data availability.* Data available upon request.

## References

Aguilera, A., Distéfano, A., Jauzein, C., Correa-Aragunde, N., Martinez, D., Martin, M. V., and Sueldo, D. J.: Do photosynthetic cells communicate with each other during cell death? From cyanobacteria to vascular plants, *Journal of Experimental Botany*, 73, 7219–7242, <https://doi.org/10.1093/jxb/erac363>, 2022.  
570

Aiken, A. C., DeCarlo, P. F., Kroll, J. H., Worsnop, D. R., Huffman, J. A., Docherty, K. S., Ulbrich, I. M., Mohr, C., Kimmel, J. R., Sueper, D., Sun, Y., Zhang, Q., Trimborn, A., Northway, M., Ziemann, P. J., Canagaratna, M. R., Onasch, T. B., Alfarra, M. R., Prevot, A. S. H., Dommen, J., Duplissy, J., Metzger, A., Baltensperger, U., and Jimenez, J. L.: O/C and OM/OC Ratios of Primary, Secondary, and Ambient Organic Aerosols with High-Resolution Time-of-Flight Aerosol Mass Spectrometry, *Environ. Sci. Technol.*, 42, 4478–4485, <https://doi.org/10.1021/es703009q>, 2008.  
575

Alsante, A. N., Thornton, D. C. O., and Brooks, S. D.: Ocean Aerobiology, *Front. Microbiol.*, 12, 764178, <https://doi.org/10.3389/fmicb.2021.764178>, 2021.  
580

Asch, R. G., Stock, C. A., and Sarmiento, J. L.: Climate change impacts on mismatches between phytoplankton blooms and fish spawning phenology, *Global Change Biology*, 25, 2544–2559, <https://doi.org/10.1111/gcb.14650>, 2019.



- 585 Baer, S. E., Lomas, M. W., Terpis, K. X., Mougnot, C., and Martiny, A. C.: Stoichiometry of *Prochlorococcus*, *Synechococcus*, and small eukaryotic populations in the western North Atlantic Ocean, *Environmental Microbiology*, 19, 1568–1583, <https://doi.org/10.1111/1462-2920.13672>, 2017.
- 590 Bahadur, R., Uplinger, T., Russell, L. M., Sive, B. C., Cliff, S. S., Millet, D. B., Goldstein, A., and Bates, T. S.: Phenol Groups in Northeastern U.S. Submicrometer Aerosol Particles Produced from Seawater Sources, *Environ. Sci. Technol.*, 44, 2542–2548, <https://doi.org/10.1021/es9032277>, 2010.
- Ban, Z., Hu, X., and Li, J.: Tipping points of marine phytoplankton to multiple environmental stressors, *Nat. Clim. Chang.*, 12, 1045–1051, <https://doi.org/10.1038/s41558-022-01489-0>, 2022.
- 595 Bates, T. S., Quinn, P. K., Frossard, A. A., Russell, L. M., Hakala, J., Petäjä, T., Kulmala, M., Covert, D. S., Cappa, C. D., Li, S.-M., Hayden, K. L., Nuaaman, I., McLaren, R., Massoli, P., Canagaratna, M. R., Onasch, T. B., Sueper, D., Worsnop, D. R., and Keene, W. C.: Measurements of ocean derived aerosol off the coast of California: MEASUREMENTS OF OCEAN DERIVED AEROSOL, *J. Geophys. Res.*, 117, n/a-n/a, <https://doi.org/10.1029/2012JD017588>, 2012.
- 600 Becagli, S., Lazzara, L., Marchese, C., Dayan, U., Ascanius, S. E., Cacciani, M., Caiazza, L., Di Biagio, C., Di Iorio, T., Di Sarra, A., Eriksen, P., Fani, F., Giardi, F., Meloni, D., Muscari, G., Pace, G., Severi, M., Traversi, R., and Udisti, R.: Relationships linking primary production, sea ice melting, and biogenic aerosol in the Arctic, *Atmospheric Environment*, 136, 1–15, <https://doi.org/10.1016/j.atmosenv.2016.04.002>, 2016.
- 605 Bedford, J., Ostle, C., Johns, D. G., Atkinson, A., Best, M., Bresnan, E., Machairopoulou, M., Graves, C. A., Devlin, M., Milligan, A., Pitois, S., Mellor, A., Tett, P., and McQuatters-Gollop, A.: Lifeform indicators reveal large-scale shifts in plankton across the North-West European shelf, *Global Change Biology*, 26, 3482–3497, <https://doi.org/10.1111/gcb.15066>, 2020.
- Behrendt, S., Dimpfl, T., Peter, F. J., and Zimmermann, D. J.: RTransferEntropy — Quantifying information flow between different time series using effective transfer entropy, *SoftwareX*, 10, 100265, <https://doi.org/10.1016/j.softx.2019.100265>, 2019.
- 610 Behrenfeld, M. J., Moore, R. H., Hostetler, C. A., Graff, J., Gaube, P., Russell, L. M., Chen, G., Doney, S. C., Giovannoni, S., Liu, H., Proctor, C., Bolaños, L. M., Baetge, N., Davie-Martin, C., Westberry, T. K., Bates, T. S., Bell, T. G., Bidle, K. D., Boss, E. S., Brooks, S. D., Cairns, B., Carlson, C., Halsey, K., Harvey, E. L., Hu, C., Karp-Boss, L., Kleb, M., Menden-Deuer, S., Morison, F., Quinn, P. K., Scarino, A. J., Anderson, B., Chowdhary, J., Crosbie, E., Ferrare, R., Hair, J. W., Hu, Y., Janz, S., Redemann, J., 615 Saltzman, E., Shook, M., Siegel, D. A., Wisthaler, A., Martin, M. Y., and Ziemba, L.: The North Atlantic Aerosol and Marine Ecosystem Study (NAAMES): Science Motive and Mission Overview, *Front. Mar. Sci.*, 6, 122, <https://doi.org/10.3389/fmars.2019.00122>, 2019.
- 620 Bell, T. G., Porter, J. G., Wang, W.-L., Lawler, M. J., Boss, E., Behrenfeld, M. J., and Saltzman, E. S.: Predictability of Seawater DMS During the North Atlantic Aerosol and Marine Ecosystem Study (NAAMES), *Front. Mar. Sci.*, 7, 596763, <https://doi.org/10.3389/fmars.2020.596763>, 2021.
- 625 Bellouin, N., Quaas, J., Gryspeerdt, E., Kinne, S., Stier, P., Watson-Parris, D., Boucher, O., Carslaw, K. S., Christensen, M., Daniau, A. -L., Dufresne, J. -L., Feingold, G., Fiedler, S., Forster, P., Gettelman, A., Haywood, J. M., Lohmann, U., Malavelle, F., Mauritsen, T., McCoy, D. T., Myhre, G., Mülmenstädt, J., Neubauer, D., Possner, A., Rugenstein, M., Sato, Y., Schulz, M., Schwartz, S. E., Sourdeval, O., Storelvmo, T., Toll, V., Winker, D., and Stevens, B.: Bounding Global Aerosol Radiative Forcing of Climate Change, *Rev. Geophys.*, 58, <https://doi.org/10.1029/2019RG000660>, 2020.



- 630 Benavent, N., Mahajan, A. S., Li, Q., Cuevas, C. A., Schmale, J., Angot, H., Jokinen, T., Quéléver, L. L. J., Blechschmidt, A.-M., Zilker, B., Richter, A., Serna, J. A., Garcia-Nieto, D., Fernandez, R. P., Skov, H., Dumitrascu, A., Simões Pereira, P., Abrahamsson, K., Bucci, S., Duetsch, M., Stohl, A., Beck, I., Laurila, T., Blomquist, B., Howard, D., Archer, S. D., Bariteau, L., Helmig, D., Hueber, J., Jacobi, H.-W., Posman, K., Dada, L., Daellenbach, K. R., and Saiz-Lopez, A.: Substantial contribution of iodine to Arctic ozone destruction, *Nat. Geosci.*, <https://doi.org/10.1038/s41561-022-01018-w>, 2022.
- Bigg, E. K. and Leck, C.: The composition of fragments of bubbles bursting at the ocean surface, *J. Geophys. Res.*, 113, D11209, <https://doi.org/10.1029/2007JD009078>, 2008.
- 635 Boyd, C. M., Sanchez, J., Xu, L., Eugene, A. J., Nah, T., Tuet, W. Y., Guzman, M. I., and Ng, N. L.: Secondary organic aerosol formation from the  $\beta$ -pinene+NO<sub>2</sub> system: effect of humidity and peroxy radical fate, *Atmos. Chem. Phys.*, 15, 7497–7522, <https://doi.org/10.5194/acp-15-7497-2015>, 2015.
- 640 Brüggemann, M., Hayeck, N., and George, C.: Interfacial photochemistry at the ocean surface is a global source of organic vapors and aerosols, *Nat Commun*, 9, 2101, <https://doi.org/10.1038/s41467-018-04528-7>, 2018.
- Canagaratna, M. R., Jayne, J. T., Jimenez, J. L., Allan, J. D., Alfarra, M. R., Zhang, Q., Onasch, T. B., Drewnick, F., Coe, H., Middlebrook, A., Delia, A., Williams, L. R., Trimborn, A. M., Northway, M. J., DeCarlo, P. F., Kolb, C. E., Davidovits, P., and Worsnop, D. R.: Chemical and microphysical characterization of ambient aerosols with the aerodyne aerosol mass spectrometer, *Mass Spectrom. Rev.*, 26, 185–222, <https://doi.org/10.1002/mas.20115>, 2007.
- 645 Canagaratna, M. R., Jimenez, J. L., Kroll, J. H., Chen, Q., Kessler, S. H., Massoli, P., Hildebrandt Ruiz, L., Fortner, E., Williams, L. R., Wilson, K. R., Surratt, J. D., Donahue, N. M., Jayne, J. T., and Worsnop, D. R.: Elemental ratio measurements of organic compounds using aerosol mass spectrometry: characterization, improved calibration, and implications, *Atmos. Chem. Phys.*, 15, 253–272, <https://doi.org/10.5194/acp-15-253-2015>, 2015.
- 650 Canonaco, F., Crippa, M., Slowik, J. G., Baltensperger, U., and Prévôt, A. S. H.: SoFi, an IGOR-based interface for the efficient use of the generalized multilinear engine (ME-2) for the source apportionment: ME-2 application to aerosol mass spectrometer data, *Atmos. Meas. Tech.*, 6, 3649–3661, <https://doi.org/10.5194/amt-6-3649-2013>, 2013.
- 655 Canonaco, F., Tobler, A., Chen, G., Sosedova, Y., Slowik, J. G., Bozzetti, C., Daellenbach, K. R., El Haddad, I., Crippa, M., Huang, R.-J., Furger, M., Baltensperger, U., and Prévôt, A. S. H.: A new method for long-term source apportionment with time-dependent factor profiles and uncertainty assessment using SoFi Pro: application to 1 year of organic aerosol data, *Atmos. Meas. Tech.*, 14, 923–943, <https://doi.org/10.5194/amt-14-923-2021>, 2021.
- 660 Carslaw, K. S., Gordon, H., Hamilton, D. S., Johnson, J. S., Regayre, L. A., Yoshioka, M., and Pringle, K. J.: Aerosols in the Pre-industrial Atmosphere, *Curr Clim Change Rep*, 3, 1–15, <https://doi.org/10.1007/s40641-017-0061-2>, 2017.
- Cavalli, F.: Advances in characterization of size-resolved organic matter in marine aerosol over the North Atlantic, *J. Geophys. Res.*, 109, D24215, <https://doi.org/10.1029/2004JD005137>, 2004.
- 665 Cerfonteyn, M., Groben, R., Vaulot, D., Guðmundsson, K., Vannier, P., Pérez-Hernández, M. D., and Marteinsson, V. Þ.: The distribution and diversity of eukaryotic phytoplankton in the Icelandic marine environment, *Sci Rep*, 13, 8519, <https://doi.org/10.1038/s41598-023-35537-2>, 2023.



- 670 Choi, J. H., Jang, E., Yoon, Y. J., Park, J. Y., Kim, T. -W., Becagli, S., Caiazzo, L., Cappelletti, D., Krejci, R., Eleftheriadis, K., Park, K. -T., and Jang, K. S.: Influence of Biogenic Organics on the Chemical Composition of Arctic Aerosols, *Global Biogeochemical Cycles*, 33, 1238–1250, <https://doi.org/10.1029/2019GB006226>, 2019.
- 675 Cochran, R. E., Laskina, O., Trueblood, J. V., Estillore, A. D., Morris, H. S., Jayarathne, T., Sultana, C. M., Lee, C., Lin, P., Laskin, J., Laskin, A., Dowling, J. A., Qin, Z., Cappa, C. D., Bertram, T. H., Tivanski, A. V., Stone, E. A., Prather, K. A., and Grassian, V. H.: Molecular Diversity of Sea Spray Aerosol Particles: Impact of Ocean Biology on Particle Composition and Hygroscopicity, *Chem*, 2, 655–667, <https://doi.org/10.1016/j.chempr.2017.03.007>, 2017.
- 680 Crippa, M., El Haddad, I., Slowik, J. G., DeCarlo, P. F., Mohr, C., Heringa, M. F., Chirico, R., Marchand, N., Sciare, J., Baltensperger, U., and Prévôt, A. S. H.: Identification of marine and continental aerosol sources in Paris using high resolution aerosol mass spectrometry: AEROSOL SOURCES IN PARIS USING HR-TOF-MS, *J. Geophys. Res. Atmos.*, 118, 1950–1963, <https://doi.org/10.1002/jgrd.50151>, 2013.
- 685 Croft, B., Martin, R. V., Moore, R. H., Ziemba, L. D., Crosbie, E. C., Liu, H., Russell, L. M., Saliba, G., Wisthaler, A., Müller, M., Schiller, A., Galí, M., Chang, R. Y.-W., McDuffie, E. E., Bilsback, K. R., and Pierce, J. R.: Factors controlling marine aerosol size distributions and their climate effects over the northwest Atlantic Ocean region, *Atmos. Chem. Phys.*, 21, 1889–1916, <https://doi.org/10.5194/acp-21-1889-2021>, 2021.
- 690 Cubison, M. J., Ortega, A. M., Hayes, P. L., Farmer, D. K., Day, D., Lechner, M. J., Brune, W. H., Apel, E., Diskin, G. S., Fisher, J. A., Fuelberg, H. E., Hecobian, A., Knapp, D. J., Mikoviny, T., Riemer, D., Sachse, G. W., Sessions, W., Weber, R. J., Weinheimer, A. J., Wisthaler, A., and Jimenez, J. L.: Effects of aging on organic aerosol from open biomass burning smoke in aircraft and laboratory studies, *Atmos. Chem. Phys.*, 11, 12049–12064, <https://doi.org/10.5194/acp-11-12049-2011>, 2011.
- 695 Cui, S., Huang, D. D., Wu, Y., Wang, J., Shen, F., Xian, J., Zhang, Y., Wang, H., Huang, C., Liao, H., and Ge, X.: Chemical properties, sources and size-resolved hygroscopicity of submicron black-carbon-containing aerosols in urban Shanghai, *Atmos. Chem. Phys.*, 22, 8073–8096, <https://doi.org/10.5194/acp-22-8073-2022>, 2022.
- 700 Dada, L., Angot, H., Beck, I., Baccharini, A., Quéléver, L. L. J., Boyer, M., Laurila, T., Brasseur, Z., Jozef, G., De Boer, G., Shupe, M. D., Henning, S., Bucci, S., Dütsch, M., Stohl, A., Petäjä, T., Daellenbach, K. R., Jokinen, T., and Schmale, J.: A central arctic extreme aerosol event triggered by a warm air-mass intrusion, *Nat Commun*, 13, 5290, <https://doi.org/10.1038/s41467-022-32872-2>, 2022.
- 705 DeCarlo, P. F., Kimmel, J. R., Trimborn, A., Northway, M. J., Jayne, J. T., Aiken, A. C., Gonin, M., Fuhrer, K., Horvath, T., Docherty, K. S., Worsnop, D. R., and Jimenez, J. L.: Field-Deployable, High-Resolution, Time-of-Flight Aerosol Mass Spectrometer, *Anal. Chem.*, 78, 8281–8289, <https://doi.org/10.1021/ac061249n>, 2006.
- 705 Decesari, S., Mircea, M., Cavalli, F., Fuzzi, S., Moretti, F., Tagliavini, E., and Facchini, M. C.: Source Attribution of Water-Soluble Organic Aerosol by Nuclear Magnetic Resonance Spectroscopy, *Environ. Sci. Technol.*, 41, 2479–2484, <https://doi.org/10.1021/es061711l>, 2007.
- Derwent, R. G., Simmonds, P. G., and Collins, W. J.: Ozone and carbon monoxide measurements at a remote maritime location, mace head, Ireland, from 1990 to 1992, *Atmospheric Environment*, 28, 2623–2637, [https://doi.org/10.1016/1352-2310\(94\)90436-7](https://doi.org/10.1016/1352-2310(94)90436-7), 1994.



- 710 Derwent, R. G., Manning, A. J., Simmonds, P. G., Spain, T. G., and O'Doherty, S.: Long-term trends in ozone in baseline and European regionally-polluted air at Mace Head, Ireland over a 30-year period, *Atmospheric Environment*, 179, 279–287, <https://doi.org/10.1016/j.atmosenv.2018.02.024>, 2018.
- Dominutti, P. A., Chevassus, E., Baray, J.-L., Jaffrezo, J.-L., Borbon, A., Colomb, A., Deguillaume, L., El Gdachi, S., Houdier, S., Leriche, M., Metzger, J.-M., Rocco, M., Tulet, P., Sellegri, K., and Freney, E.:  
715 Evaluation of the Sources, Precursors, and Processing of Aerosols at a High-Altitude Tropical Site, *ACS Earth Space Chem.*, 6, 2412–2431, <https://doi.org/10.1021/acsearthspacechem.2c00149>, 2022.
- Drewnick, F., Hings, S. S., Alfarra, M. R., Prevot, A. S. H., and Borrmann, S.: Aerosol quantification with the Aerodyne Aerosol Mass Spectrometer: detection limits and ionizer background effects, *Atmos. Meas. Tech.*, 2, 33–46, <https://doi.org/10.5194/amt-2-33-2009>, 2009.
- 720 Duplissy, J., DeCarlo, P. F., Dommen, J., Alfarra, M. R., Metzger, A., Barmapadimos, I., Prevot, A. S. H., Weingartner, E., Tritscher, T., Gysel, M., Aiken, A. C., Jimenez, J. L., Canagaratna, M. R., Worsnop, D. R., Collins, D. R., Tomlinson, J., and Baltensperger, U.: Relating hygroscopicity and composition of organic aerosol particulate matter, *Atmos. Chem. Phys.*, 11, 1155–1165, <https://doi.org/10.5194/acp-11-1155-2011>, 2011.
- 725 Edtbauer, A., Stöner, C., Pfannerstill, E. Y., Berasategui, M., Walter, D., Crowley, J. N., Lelieveld, J., and Williams, J.: A new marine biogenic emission: methane sulfonamide (MSAM), dimethyl sulfide (DMS), and dimethyl sulfone (DMSO) measured in air over the Arabian Sea, *Atmos. Chem. Phys.*, 20, 6081–6094, <https://doi.org/10.5194/acp-20-6081-2020>, 2020.
- 730 Etminan, M., Myhre, G., Highwood, E. J., and Shine, K. P.: Radiative forcing of carbon dioxide, methane, and nitrous oxide: A significant revision of the methane radiative forcing, *Geophys. Res. Lett.*, 43, <https://doi.org/10.1002/2016GL071930>, 2016.
- Facchini, M. C., Rinaldi, M., Decesari, S., Carbone, C., Finessi, E., Mircea, M., Fuzzi, S., Ceburnis, D., Flanagan, R., Nilsson, E. D., de Leeuw, G., Martino, M., Woeltjen, J., and O'Dowd, C. D.: Primary submicron marine aerosol dominated by insoluble organic colloids and aggregates, *Geophys. Res. Lett.*, 35, L17814, <https://doi.org/10.1029/2008GL034210>, 2008.
- 735 Faiola, C. L., Wen, M., and VanReken, T. M.: Chemical characterization of biogenic secondary organic aerosol generated from plant emissions under baseline and stressed conditions: inter- and intra-species variability for six coniferous species, *Atmos. Chem. Phys.*, 15, 3629–3646, <https://doi.org/10.5194/acp-15-3629-2015>, 2015.
- 740 Flerus, R., Lechtenfeld, O. J., Koch, B. P., McCallister, S. L., Schmitt-Kopplin, P., Benner, R., Kaiser, K., and Kattner, G.: A molecular perspective on the ageing of marine dissolved organic matter, *Biogeosciences*, 9, 1935–1955, <https://doi.org/10.5194/bg-9-1935-2012>, 2012.
- Fossum, K. N., Ovadnevaite, J., Ceburnis, D., Dall'Osto, M., Marullo, S., Bellacicco, M., Simó, R., Liu, D., Flynn, M., Zuend, A., and O'Dowd, C.: Summertime Primary and Secondary Contributions to Southern  
745 Ocean Cloud Condensation Nuclei, *Sci Rep*, 8, 13844, <https://doi.org/10.1038/s41598-018-32047-4>, 2018.
- Glicker, H. S., Lawler, M. J., Chee, S., Resch, J., Garofalo, L. A., Mayer, K. J., Prather, K. A., Farmer, D. K., and Smith, J. N.: Chemical Composition of an Ultrafine Sea Spray Aerosol during the Sea Spray Chemistry and Particle Evolution Experiment, *ACS Earth Space Chem.*, 6, 1914–1923,  
750 <https://doi.org/10.1021/acsearthspacechem.2c00127>, 2022.



- Goldstein, A. H. and Galbally, I. E.: Known and Unexplored Organic Constituents in the Earth's Atmosphere, *Environ. Sci. Technol.*, 41, 1514–1521, <https://doi.org/10.1021/es072476p>, 2007.
- 755 Grigas, T., Ovadnevaite, J., Ceburnis, D., Moran, E., McGovern, F. M., Jennings, S. G., and O'Dowd, C.: Sophisticated Clean Air Strategies Required to Mitigate Against Particulate Organic Pollution, *Sci Rep*, 7, 44737, <https://doi.org/10.1038/srep44737>, 2017.
- Gryspeerd, E., Povey, A. C., Grainger, R. G., Hasekamp, O., Hsu, N. C., Mulcahy, J. P., Sayer, A. M., and Sorooshian, A.: Uncertainty in aerosol–cloud radiative forcing is driven by clean conditions, *Atmos. Chem. Phys.*, 23, 4115–4122, <https://doi.org/10.5194/acp-23-4115-2023>, 2023.
- 760 Guo, J., Zhang, J., Yang, K., Liao, H., Zhang, S., Huang, K., Lv, Y., Shao, J., Yu, T., Tong, B., Li, J., Su, T., Yim, S. H. L., Stoffelen, A., Zhai, P., and Xu, X.: Investigation of near-global daytime boundary layer height using high-resolution radiosondes: first results and comparison with ERA5, MERRA-2, JRA-55, and NCEP-2 reanalyses, *Atmos. Chem. Phys.*, 21, 17079–17097, <https://doi.org/10.5194/acp-21-17079-2021>, 2021.
- 765 Han, S., Hong, J., Luo, Q., Xu, H., Tan, H., Wang, Q., Tao, J., Zhou, Y., Peng, L., He, Y., Shi, J., Ma, N., Cheng, Y., and Su, H.: Hygroscopicity of organic compounds as a function of organic functionality, water solubility, molecular weight, and oxidation level, *Atmos. Chem. Phys.*, 22, 3985–4004, <https://doi.org/10.5194/acp-22-3985-2022>, 2022.
- 770 Hátún, H., Lohmann, K., Matei, D., Jungclaus, J. H., Pacariz, S., Bersch, M., Gislason, A., Ólafsson, J., and Reid, P. C.: An inflated subpolar gyre blows life toward the northeastern Atlantic, *Progress in Oceanography*, 147, 49–66, <https://doi.org/10.1016/j.pocean.2016.07.009>, 2016.
- Håvik, L. and Våge, K.: Wind-Driven Coastal Upwelling and Downwelling in the Shelfbreak East Greenland Current, *JGR Oceans*, 123, 6106–6115, <https://doi.org/10.1029/2018JC014273>, 2018.
- 775 Holland, M. M., Louchart, A., Artigas, L. F., Ostle, C., Atkinson, A., Rombouts, I., Graves, C. A., Devlin, M., Heyden, B., Machairopoulou, M., Bresnan, E., Schilder, J., Jakobsen, H. H., Lloyd-Hartley, H., Tett, P., Best, M., Goberville, E., and McQuatters-Gollop, A.: Major declines in NE Atlantic plankton contrast with more stable populations in the rapidly warming North Sea, *Science of The Total Environment*, 898, 165505, <https://doi.org/10.1016/j.scitotenv.2023.165505>, 2023.
- 780 Hu, W. W., Campuzano-Jost, P., Palm, B. B., Day, D. A., Ortega, A. M., Hayes, P. L., Krechmer, J. E., Chen, Q., Kuwata, M., Liu, Y. J., de Sá, S. S., McKinney, K., Martin, S. T., Hu, M., Budisulistiorini, S. H., Riva, M., Surratt, J. D., St. Clair, J. M., Isaacman-Van Wertz, G., Yee, L. D., Goldstein, A. H., Carbone, S., Brito, J., Artaxo, P., de Gouw, J. A., Koss, A., Wisthaler, A., Mikoviny, T., Karl, T., Kaser, L., Jud, W., Hansel, A., Docherty, K. S., Alexander, M. L., Robinson, N. H., Coe, H., Allan, J. D., Canagaratna, M. R., Paulot, F., and Jimenez, J. L.: Characterization of a real-time tracer for isoprene epoxydiols-derived secondary organic aerosol (IEPOX-SOA) from aerosol mass spectrometer measurements, *Atmos. Chem. Phys.*, 15, 11807–11833, <https://doi.org/10.5194/acp-15-11807-2015>, 2015.
- 785 Huang, S., Wu, Z., Poulain, L., van Pinxteren, M., Merkel, M., Assmann, D., Herrmann, H., and Wiedensohler, A.: Source apportionment of the organic aerosol over the Atlantic Ocean from 53° N to 53° S: significant contributions from marine emissions and long-range transport, *Atmos. Chem. Phys.*, 18, 18043–18062, <https://doi.org/10.5194/acp-18-18043-2018>, 2018.
- 790 Huffman, J. A., Jayne, J. T., Drewnick, F., Aiken, A. C., Onasch, T., Worsnop, D. R., and Jimenez, J. L.: Design, Modeling, Optimization, and Experimental Tests of a Particle Beam Width Probe for the Aerodyne Aerosol Mass Spectrometer, *Aerosol Science and Technology*, 39, 1143–1163, <https://doi.org/10.1080/02786820500423782>, 2005.





- 795 Jang, J., Park, J., Park, J., Yoon, Y. J., Dall&apos;Osto, M. s., Park, K.-T., Jang, E., Lee, J., Cho, K. H., and Lee, B. Y.: Ocean-Atmosphere Interactions: Different Organic Components Across Pacific and Southern Oceans, *SSRN Journal*, <https://doi.org/10.2139/ssrn.4290253>, 2022.
- Karl, M., Leck, C., Coz, E., and Heintzenberg, J.: Marine nanogels as a source of atmospheric nanoparticles in the high Arctic, *Geophys. Res. Lett.*, **40**, 3738–3743, <https://doi.org/10.1002/grl.50661>, 2013.
- 800 King, S. M., Butcher, A. C., Rosenoern, T., Coz, E., Lieke, K. I., De Leeuw, G., Nilsson, E. D., and Bilde, M.: Investigating Primary Marine Aerosol Properties: CCN Activity of Sea Salt and Mixed Inorganic–Organic Particles, *Environ. Sci. Technol.*, **46**, 10405–10412, <https://doi.org/10.1021/es300574u>, 2012.
- 805 Kirkby, J., Duplissy, J., Sengupta, K., Frege, C., Gordon, H., Williamson, C., Heinritzi, M., Simon, M., Yan, C., Almeida, J., Tröstl, J., Nieminen, T., Ortega, I. K., Wagner, R., Adamov, A., Amorim, A., Bernhammer, A.-K., Bianchi, F., Breitenlechner, M., Brilke, S., Chen, X., Craven, J., Dias, A., Ehrhart, S., Flagan, R. C., Franchin, A., Fuchs, C., Guida, R., Hakala, J., Hoyle, C. R., Jokinen, T., Junninen, H., Kangasluoma, J., Kim, J., Krapf, M., Kürten, A., Laaksonen, A., Lehtipalo, K., Makhmutov, V., Mathot, S., Molteni, U., Onnela, A., Peräkylä, O., Piel, F., Petäjä, T., Praplan, A. P., Pringle, K., Rap, A., Richards, N. A. D., Riipinen, I., Rissanen, M. P., Rondo, L., Sarnela, N., Schobesberger, S., Scott, C. E., Seinfeld, J. H., Sipilä, M., Steiner, G., Stozhkov, Y., Stratmann, F., Tomé, A., Virtanen, A., Vogel, A. L., Wagner, A. C., Wagner, P. E., Weingartner, E., Wimmer, D., Winkler, P. M., Ye, P., Zhang, X., Hansel, A., Dommen, J., Donahue, N. M., Worsnop, D. R., Baltensperger, U., Kulmala, M., Carslaw, K. S., and Curtius, J.: Ion-induced nucleation of pure biogenic particles, *Nature*, **533**, 521–526, <https://doi.org/10.1038/nature17953>, 2016.
- 815 Kołodziejczyk, A., Pyrcz, P., Pobudkowska, A., Błaziak, K., and Szmigielski, R.: Physicochemical Properties of Pinic, Pinonic, Norpinic, and Norpinonic Acids as Relevant  $\alpha$ -Pinene Oxidation Products, *J. Phys. Chem. B*, **123**, 8261–8267, <https://doi.org/10.1021/acs.jpcc.9b05211>, 2019.
- 820 Koteska, D., Sanchez Garcia, S., Wagner-Döbler, I., and Schulz, S.: Identification of Volatiles of the Dinoflagellate *Prorocentrum cordatum*, *Marine Drugs*, **20**, 371, <https://doi.org/10.3390/md20060371>, 2022.
- 825 Landwehr, S., Volpi, M., Haumann, F. A., Robinson, C. M., Thurnherr, I., Ferracci, V., Baccarini, A., Thomas, J., Gorodetskaya, I., Tatzelt, C., Henning, S., Modini, R. L., Forrer, H. J., Lin, Y., Cassar, N., Simó, R., Hassler, C., Moallemi, A., Fawcett, S. E., Harris, N., Airs, R., Derkani, M. H., Alberello, A., Toffoli, A., Chen, G., Rodríguez-Ros, P., Zamanillo, M., Cortés-Greus, P., Xue, L., Bolas, C. G., Leonard, K. C., Perez-Cruz, F., Walton, D., and Schmale, J.: Exploring the coupled ocean and atmosphere system with a data science approach applied to observations from the Antarctic Circumnavigation Expedition, *Earth Syst. Dynam.*, **12**, 1295–1369, <https://doi.org/10.5194/esd-12-1295-2021>, 2021.
- 830 Laskin, A., Laskin, J., and Nizkorodov, S. A.: Mass spectrometric approaches for chemical characterisation of atmospheric aerosols: critical review of the most recent advances, *Environ. Chem.*, **9**, 163, <https://doi.org/10.1071/EN12052>, 2012.
- Lawler, M. J., Schill, G. P., Brock, C. A., Froyd, K. D., Williamson, C., Kupc, A., and Murphy, D. M.: Sea Spray Aerosol Over the Remote Oceans Has Low Organic Content, *AGU Advances*, **5**, e2024AV001215, <https://doi.org/10.1029/2024AV001215>, 2024.
- 835 Lee, H. D., Morris, H. S., Laskina, O., Sultana, C. M., Lee, C., Jayarathne, T., Cox, J. L., Wang, X., Hasenecz, E. S., DeMott, P. J., Bertram, T. H., Cappa, C. D., Stone, E. A., Prather, K. A., Grassian, V. H., and Tivanski, A. V.: Organic Enrichment, Physical Phase State, and Surface Tension Depression of



Nascent Core–Shell Sea Spray Aerosols during Two Phytoplankton Blooms, *ACS Earth Space Chem.*, 4, 650–660, <https://doi.org/10.1021/acsearthspacechem.0c00032>, 2020.

- 840 Lehahn, Y., Koren, I., Schatz, D., Frada, M., Sheyn, U., Boss, E., Efrati, S., Rudich, Y., Trainic, M., Sharoni, S., Laber, C., DiTullio, G. R., Coolen, M. J. L., Martins, A. M., Van Mooy, B. A. S., Bidle, K. D., and Vardi, A.: Decoupling Physical from Biological Processes to Assess the Impact of Viruses on a Mesoscale Algal Bloom, *Current Biology*, 24, 2041–2046, <https://doi.org/10.1016/j.cub.2014.07.046>, 2014.
- 845 Lewis, S. L., Saliba, G., Russell, L. M., Quinn, P. K., Bates, T. S., and Behrenfeld, M. J.: Seasonal Differences in Submicron Marine Aerosol Particle Organic Composition in the North Atlantic, *Front. Mar. Sci.*, 8, 720208, <https://doi.org/10.3389/fmars.2021.720208>, 2021.
- Li, Y., Bai, B., Dykema, J., Shin, N., Lambe, A. T., Chen, Q., Kuwata, M., Ng, N. L., Keutsch, F. N., and Liu, P.: Predicting Real Refractive Index of Organic Aerosols From Elemental Composition, *Geophysical Research Letters*, 50, e2023GL103446, <https://doi.org/10.1029/2023GL103446>, 2023.
- 850 Lin, C., Ceburnis, D., Hellebust, S., Buckley, P., Wenger, J., Canonaco, F., Prévôt, A. S. H., Huang, R.-J., O’Dowd, C., and Ovadnevaite, J.: Characterization of Primary Organic Aerosol from Domestic Wood, Peat, and Coal Burning in Ireland, *Environ. Sci. Technol.*, 51, 10624–10632, <https://doi.org/10.1021/acs.est.7b01926>, 2017.
- 855 Liu, M. and Matsui, H.: Secondary Organic Aerosol Formation Regulates Cloud Condensation Nuclei in the Global Remote Troposphere, *Geophysical Research Letters*, 49, <https://doi.org/10.1029/2022GL100543>, 2022.
- Liu, Y., Ma, C., and Sun, J.: Integrated FT-ICR MS and metabolome reveals diatom-derived organic matter by bacterial transformation under warming and acidification, *iScience*, 26, 106812, <https://doi.org/10.1016/j.isci.2023.106812>, 2023.
- 860 Long, Y., Zhang, W., Sun, N., Zhu, P., Yan, J., and Yin, S.: Sequential Interaction of Biogenic Volatile Organic Compounds and SOAs in Urban Forests Revealed Using Toeplitz Inverse Covariance-Based Clustering and Causal Inference, *Forests*, 14, 1617, <https://doi.org/10.3390/f14081617>, 2023.
- 865 Mansour, K., Decesari, S., Facchini, M. C., Belosi, F., Paglione, M., Sandrini, S., Bellacicco, M., Marullo, S., Santoleri, R., Ovadnevaite, J., Ceburnis, D., O’Dowd, C., Roberts, G., Sanchez, K., and Rinaldi, M.: Linking Marine Biological Activity to Aerosol Chemical Composition and Cloud-Relevant Properties Over the North Atlantic Ocean, *J. Geophys. Res. Atmos.*, 125, <https://doi.org/10.1029/2019JD032246>, 2020.
- 870 Mansour, K., Decesari, S., Ceburnis, D., Ovadnevaite, J., and Rinaldi, M.: Machine learning for prediction of daily sea surface dimethylsulfide concentration and emission flux over the North Atlantic Ocean (1998–2021), *Science of The Total Environment*, 871, 162123, <https://doi.org/10.1016/j.scitotenv.2023.162123>, 2023.
- 875 Marais, E. A., Jacob, D. J., Jimenez, J. L., Campuzano-Jost, P., Day, D. A., Hu, W., Krechmer, J., Zhu, L., Kim, P. S., Miller, C. C., Fisher, J. A., Travis, K., Yu, K., Hanisco, T. F., Wolfe, G. M., Arkinson, H. L., Pyy, H. O. T., Froyd, K. D., Liao, J., and McNeill, V. F.: Aqueous-phase mechanism for secondary organic aerosol formation from isoprene: application to the southeast United States and co-benefit of SO<sub>2</sub> and NO<sub>2</sub> emission controls, *Atmos. Chem. Phys.*, 16, 1603–1618, <https://doi.org/10.5194/acp-16-1603-2016>, 2016.



- 880 Markuszewski, P., Nilsson, E. D., Zinke, J., Mårtensson, E. M., Salter, M., Makuch, P., Kitowska, M., Niedźwiecka-Wróbel, I., Drozdowska, V., Lis, D., Petelski, T., Ferrero, L., and Piskozub, J.: Multi-year gradient measurements of sea spray fluxes over the Baltic Sea and the North Atlantic Ocean, <https://doi.org/10.5194/egusphere-2024-1254>, 3 June 2024.
- 885 Mayer, K. J., Wang, X., Santander, M. V., Mitts, B. A., Sauer, J. S., Sultana, C. M., Cappa, C. D., and Prather, K. A.: Secondary Marine Aerosol Plays a Dominant Role over Primary Sea Spray Aerosol in Cloud Formation, *ACS Cent. Sci.*, **6**, 2259–2266, <https://doi.org/10.1021/acscentsci.0c00793>, 2020.
- McNeill, V. F.: Aqueous Organic Chemistry in the Atmosphere: Sources and Chemical Processing of Organic Aerosols, *Environ. Sci. Technol.*, **49**, 1237–1244, <https://doi.org/10.1021/es5043707>, 2015.
- 890 Meador, T. B., Goldenstein, N. I., Gogou, A., Herut, B., Psarra, S., Tsagaraki, T. M., and Hinrichs, K.-U.: Planktonic Lipidome Responses to Aeolian Dust Input in Low-Biomass Oligotrophic Marine Mesocosms, *Front. Mar. Sci.*, **4**, 113, <https://doi.org/10.3389/fmars.2017.00113>, 2017.
- Middlebrook, A. M., Bahreini, R., Jimenez, J. L., and Canagaratna, M. R.: Evaluation of Composition-Dependent Collection Efficiencies for the Aerodyne Aerosol Mass Spectrometer using Field Data, *Aerosol Science and Technology*, **46**, 258–271, <https://doi.org/10.1080/02786826.2011.620041>, 2012.
- 895 Mohr, C., DeCarlo, P. F., Heringa, M. F., Chirico, R., Slowik, J. G., Richter, R., Reche, C., Alastuey, A., Querol, X., Seco, R., Peñuelas, J., Jiménez, J. L., Crippa, M., Zimmermann, R., Baltensperger, U., and Prévôt, A. S. H.: Identification and quantification of organic aerosol from cooking and other sources in Barcelona using aerosol mass spectrometer data, *Atmos. Chem. Phys.*, **12**, 1649–1665, <https://doi.org/10.5194/acp-12-1649-2012>, 2012.
- 900 Moschos, V., Dzepina, K., Bhattu, D., Lamkaddam, H., Casotto, R., Daellenbach, K. R., Canonaco, F., Rai, P., Aas, W., Becagli, S., Calzolari, G., Eleftheriadis, K., Moffett, C. E., Schnelle-Kreis, J., Severi, M., Sharma, S., Skov, H., Vestenius, M., Zhang, W., Hakola, H., Hellén, H., Huang, L., Jaffrezo, J.-L., Massling, A., Nøjgaard, J. K., Petäjä, T., Popovicheva, O., Sheesley, R. J., Traversi, R., Yttri, K. E., Schmale, J., Prévôt, A. S. H., Baltensperger, U., and El Haddad, I.: Equal abundance of summertime natural and wintertime anthropogenic Arctic organic aerosols, *Nat. Geosci.*, <https://doi.org/10.1038/s41561-021-00891-1>, 2022.
- 905 Mungall, E. L., Wong, J. P. S., and Abbatt, J. P. D.: Heterogeneous Oxidation of Particulate Methanesulfonic Acid by the Hydroxyl Radical: Kinetics and Atmospheric Implications, *ACS Earth Space Chem.*, **2**, 48–55, <https://doi.org/10.1021/acsearthspacechem.7b00114>, 2018.
- 910 Mutshinda, C. M., Finkel, Z. V., and Irwin, A. J.: Large shifts in diatom and dinoflagellate biomass in the North Atlantic over six decades, <https://doi.org/10.1101/2024.07.02.601152>, 4 July 2024.
- Narayanaswamy, B. E., Renaud, P. E., Duineveld, G. C. A., Berge, J., Lavaleye, M. S. S., Reiss, H., and Brattgard, T.: Biodiversity Trends along the Western European Margin, *PLoS ONE*, **5**, e14295, <https://doi.org/10.1371/journal.pone.0014295>, 2010.
- 915 Nault, B. A., Croteau, P., Jayne, J., Williams, A., Williams, L., Worsnop, D., Katz, E. F., DeCarlo, P. F., and Canagaratna, M.: Laboratory evaluation of organic aerosol relative ionization efficiencies in the aerodyne aerosol mass spectrometer and aerosol chemical speciation monitor, *Aerosol Science and Technology*, **57**, 981–997, <https://doi.org/10.1080/02786826.2023.2223249>, 2023.



- 920 Ng, N. L., Canagaratna, M. R., Jimenez, J. L., Chhabra, P. S., Seinfeld, J. H., and Worsnop, D. R.:  
Changes in organic aerosol composition with aging inferred from aerosol mass spectra, *Atmospheric  
Chemistry and Physics*, 11, 6465–6474, <https://doi.org/10.5194/acp-11-6465-2011>, 2011.
- Nielsen, I. E., Skov, H., Massling, A., Eriksson, A. C., Dall’Osto, M., Junninen, H., Sarnela, N., Lange, R.,  
Collier, S., Zhang, Q., Cappa, C. D., and Nøjgaard, J. K.: Biogenic and anthropogenic sources of  
925 aerosols at the High Arctic site Villum Research Station, *Atmos. Chem. Phys.*, 19, 10239–10256,  
<https://doi.org/10.5194/acp-19-10239-2019>, 2019.
- O’Dowd, C., Ceburnis, D., Ovadnevaite, J., Bialek, J., Stengel, D. B., Zacharias, M., Nitschke, U.,  
Connan, S., Rinaldi, M., Fuzzi, S., Decesari, S., Cristina Facchini, M., Marullo, S., Santoleri, R.,  
Dell’Anno, A., Corinaldesi, C., Tangherlini, M., and Danovaro, R.: Connecting marine productivity to  
930 sea-spray via nanoscale biological processes: Phytoplankton Dance or Death Disco?, *Sci Rep*, 5,  
14883, <https://doi.org/10.1038/srep14883>, 2015.
- O’Dowd, C. D., Facchini, M. C., Cavalli, F., Ceburnis, D., Mircea, M., Decesari, S., Fuzzi, S., Yoon, Y. J.,  
and Putaud, J.-P.: Biogenically driven organic contribution to marine aerosol, *Nature*, 431, 676–680,  
<https://doi.org/10.1038/nature02959>, 2004.
- Ovadnevaite, J., O’Dowd, C., Dall’Osto, M., Ceburnis, D., Worsnop, D. R., and Berresheim, H.:  
935 Detecting high contributions of primary organic matter to marine aerosol: A case study: PRIMARY  
ORGANIC MARINE AEROSOL, *Geophys. Res. Lett.*, 38, n/a-n/a,  
<https://doi.org/10.1029/2010GL046083>, 2011a.
- Ovadnevaite, J., Ceburnis, D., Martucci, G., Bialek, J., Monahan, C., Rinaldi, M., Facchini, M. C.,  
Berresheim, H., Worsnop, D. R., and O’Dowd, C.: Primary marine organic aerosol: A dichotomy of low  
940 hygroscopicity and high CCN activity: MARINE AEROSOL-CLOUD INTERACTIONS, *Geophys. Res. Lett.*,  
38, n/a-n/a, <https://doi.org/10.1029/2011GL048869>, 2011b.
- Ovadnevaite, J., Ceburnis, D., Canagaratna, M., Berresheim, H., Bialek, J., Martucci, G., Worsnop, D.  
R., and O’Dowd, C.: On the effect of wind speed on submicron sea salt mass concentrations and  
source fluxes: EFFECT OF WIND SPEED ON SEA SALT, *J. Geophys. Res.*, 117, n/a-n/a,  
945 <https://doi.org/10.1029/2011JD017379>, 2012.
- Ovadnevaite, J., Manders, A., de Leeuw, G., Ceburnis, D., Monahan, C., Partanen, A.-I., Korhonen, H.,  
and O’Dowd, C. D.: A sea spray aerosol flux parameterization encapsulating wave state, *Atmos.  
Chem. Phys.*, 14, 1837–1852, <https://doi.org/10.5194/acp-14-1837-2014>, 2014a.
- Ovadnevaite, J., Ceburnis, D., Leinert, S., Dall’Osto, M., Canagaratna, M., O’Doherty, S., Berresheim,  
950 H., and O’Dowd, C.: Submicron NE Atlantic marine aerosol chemical composition and abundance:  
Seasonal trends and air mass categorization: Seasonal Trends of Marine Aerosol, *J. Geophys. Res.  
Atmos.*, 119, 11,850-11,863, <https://doi.org/10.1002/2013JD021330>, 2014b.
- Ovadnevaite, J., Zuend, A., Laaksonen, A., Sanchez, K. J., Roberts, G., Ceburnis, D., Decesari, S.,  
Rinaldi, M., Hodas, N., Facchini, M. C., Seinfeld, J. H., and O’Dowd, C.: Surface tension prevails over  
955 solute effect in organic-influenced cloud droplet activation, *Nature*, 546, 637–641,  
<https://doi.org/10.1038/nature22806>, 2017.
- Oziel, L., Baudena, A., Ardyna, M., Massicotte, P., Randelhoff, A., Sallée, J.-B., Ingvaldsen, R. B.,  
Devred, E., and Babin, M.: Faster Atlantic currents drive poleward expansion of temperate  
960 phytoplankton in the Arctic Ocean, *Nat Commun*, 11, 1705, <https://doi.org/10.1038/s41467-020-15485-5>, 2020.



- Paatero, P.: The Multilinear Engine—A Table-Driven, Least Squares Program for Solving Multilinear Problems, Including the  $n$ -Way Parallel Factor Analysis Model, *Journal of Computational and Graphical Statistics*, 8, 854–888, <https://doi.org/10.1080/10618600.1999.10474853>, 1999.
- 965 Paatero, P. and Tapper, U.: Positive matrix factorization: A non-negative factor model with optimal utilization of error estimates of data values, *Environmetrics*, 5, 111–126, <https://doi.org/10.1002/env.3170050203>, 1994.
- Park, J., Jang, J., Yoon, Y. J., Kang, S., Kang, H., Park, K., Cho, K. H., Kim, J.-H., Dall’Osto, M., and Lee, B. Y.: When river water meets seawater: Insights into primary marine aerosol production, *Science of The Total Environment*, 807, 150866, <https://doi.org/10.1016/j.scitotenv.2021.150866>, 2022.
- 970 Peltola, M., Rose, C., Trueblood, J. V., Gray, S., Harvey, M., and Sellegri, K.: Chemical precursors of new particle formation in coastal New Zealand, *Aerosols/Field Measurements/Troposphere/Chemistry (chemical composition and reactions)*, <https://doi.org/10.5194/acp-2022-307>, 2022.
- 975 Pettersen, C., Henderson, S. A., Mattingly, K. S., Bennartz, R., and Breeden, M. L.: The Critical Role of Euro-Atlantic Blocking in Promoting Snowfall in Central Greenland, *JGR Atmospheres*, 127, e2021JD035776, <https://doi.org/10.1029/2021JD035776>, 2022.
- Preece, J. R., Mote, T. L., Cohen, J., Wachowicz, L. J., Knox, J. A., Tedesco, M., and Kooperman, G. J.: Summer atmospheric circulation over Greenland in response to Arctic amplification and diminished spring snow cover, *Nat Commun*, 14, 3759, <https://doi.org/10.1038/s41467-023-39466-6>, 2023.
- 980 Quinn, P. K., Coffman, D. J., Johnson, J. E., Upchurch, L. M., and Bates, T. S.: Small fraction of marine cloud condensation nuclei made up of sea spray aerosol, *Nature Geosci*, 10, 674–679, <https://doi.org/10.1038/ngeo3003>, 2017.
- 985 Radoman, N., Christiansen, S., Johansson, J., Hawkes, J., Bilde, M., Cousins, I. T., and Salter, M.: Probing the impact of a phytoplankton bloom on the chemistry of nascent sea spray aerosol using high-resolution mass spectrometry, *Environ. Sci.: Atmos.*, 10.1039/D2EA00028H, <https://doi.org/10.1039/D2EA00028H>, 2022.
- Rahmstorf, S., Box, J. E., Feulner, G., Mann, M. E., Robinson, A., Rutherford, S., and Schaffernicht, E. J.: Exceptional twentieth-century slowdown in Atlantic Ocean overturning circulation, *Nature Clim Change*, 5, 475–480, <https://doi.org/10.1038/nclimate2554>, 2015.
- 990 Rapf, R. J., Dooley, M. R., Kappes, K., Perkins, R. J., and Vaida, V.: pH Dependence of the Aqueous Photochemistry of  $\alpha$ -Keto Acids, *J. Phys. Chem. A*, 121, 8368–8379, <https://doi.org/10.1021/acs.jpca.7b08192>, 2017.
- 995 Rinaldi, M., Fuzzi, S., Decesari, S., Marullo, S., Santoleri, R., Provenzale, A., Von Hardenberg, J., Ceburnis, D., Vaishya, A., O’Dowd, C. D., and Facchini, M. C.: Is chlorophyll-  $a$  the best surrogate for organic matter enrichment in submicron primary marine aerosol?, *JGR Atmospheres*, 118, 4964–4973, <https://doi.org/10.1002/jgrd.50417>, 2013.
- 1000 Rinaldi, M., Paglione, M., Decesari, S., Harrison, R. M., Beddows, D. C. S., Ovadnevaite, J., Ceburnis, D., O’Dowd, C. D., Simó, R., and Dall’Osto, M.: Contribution of Water-Soluble Organic Matter from Multiple Marine Geographic Eco-Regions to Aerosols around Antarctica, *Environ. Sci. Technol.*, 54, 7807–7817, <https://doi.org/10.1021/acs.est.0c00695>, 2020.



- 1005 Robinson, N. H., Hamilton, J. F., Allan, J. D., Langford, B., Oram, D. E., Chen, Q., Docherty, K., Farmer, D. K., Jimenez, J. L., Ward, M. W., Hewitt, C. N., Barley, M. H., Jenkin, M. E., Rickard, A. R., Martin, S. T., McFiggans, G., and Coe, H.: Evidence for a significant proportion of Secondary Organic Aerosol from isoprene above a maritime tropical forest, *Atmos. Chem. Phys.*, **11**, 1039–1050, <https://doi.org/10.5194/acp-11-1039-2011>, 2011.
- Rosenfeld, D., Zhu, Y., Wang, M., Zheng, Y., Goren, T., and Yu, S.: Aerosol-driven droplet concentrations dominate coverage and water of oceanic low-level clouds, *Science*, **363**, eaav0566, <https://doi.org/10.1126/science.aav0566>, 2019.
- 1010 Rousseaux, C. S., Hirata, T., and Gregg, W. W.: Satellite views of global phytoplankton community distributions using an empirical algorithm and a numerical model, <https://doi.org/10.5194/bgd-10-1083-2013>, 24 January 2013.
- Russell, L. M., Bahadur, R., and Ziemann, P. J.: Identifying organic aerosol sources by comparing functional group composition in chamber and atmospheric particles, *Proc. Natl. Acad. Sci. U.S.A.*, **108**, 3516–3521, <https://doi.org/10.1073/pnas.1006461108>, 2011.
- 1015 S. Gerard Jennings, Christoph Kleefeld, Colin D. O’Dowd, Carsten Junker, T. Gerard Spain, Phillip O’Brien, Aodhaghan F. Roddy, and and Thomas C. O’Connor: Mace Head Atmospheric Research Station — characterization of aerosol radiative parameters, *BOREAL ENVIRONMENT RESEARCH* **8**, 2003.
- 1020 Saha, M. and Fink, P.: Algal volatiles – the overlooked chemical language of aquatic primary producers, *Biological Reviews*, **97**, 2162–2173, <https://doi.org/10.1111/brv.12887>, 2022.
- Saliba, G., Chen, C.-L., Lewis, S., Russell, L. M., Rivellini, L.-H., Lee, A. K. Y., Quinn, P. K., Bates, T. S., Haëntjens, N., Boss, E. S., Karp-Boss, L., Baetge, N., Carlson, C. A., and Behrenfeld, M. J.: Factors driving the seasonal and hourly variability of sea-spray aerosol number in the North Atlantic, *Proc Natl Acad Sci USA*, **116**, 20309–20314, <https://doi.org/10.1073/pnas.1907574116>, 2019.
- 1025 Sanchez, K. J., Zhang, B., Liu, H., Saliba, G., Chen, C.-L., Lewis, S. L., Russell, L. M., Shook, M. A., Crosbie, E. C., Ziemba, L. D., Brown, M. D., Shingler, T. J., Robinson, C. E., Wiggins, E. B., Thornhill, K. L., Winstead, E. L., Jordan, C., Quinn, P. K., Bates, T. S., Porter, J., Bell, T. G., Saltzman, E. S., Behrenfeld, M. J., and Moore, R. H.: Linking marine phytoplankton emissions, meteorological processes, and downwind particle properties with FLEXPART, *Atmos. Chem. Phys.*, **21**, 831–851, <https://doi.org/10.5194/acp-21-831-2021>, 2021.
- 1030 Sanchez, K. J., Zhang, B., Liu, H., Brown, M. D., Crosbie, E. C., Gallo, F., Hair, J. W., Hostetler, C. A., Jordan, C. E., Robinson, C. E., Scarino, A. J., Shingler, T. J., Shook, M. A., Thornhill, K. L., Wiggins, E. B., Winstead, E. L., Ziemba, L. D., Saliba, G., Lewis, S. L., Russell, L. M., Quinn, P. K., Bates, T. S., Porter, J., Bell, T. G., Gaube, P., Saltzman, E. S., Behrenfeld, M. J., and Moore, R. H.: North Atlantic Ocean SST-gradient-driven variations in aerosol and cloud evolution along Lagrangian cold-air outbreak trajectories, *Atmos. Chem. Phys.*, **22**, 2795–2815, <https://doi.org/10.5194/acp-22-2795-2022>, 2022.
- 1035 Sanders, R. N. C., Jones, D. C., Josey, S. A., Sinha, B., and Forget, G.: Causes of the 2015 North Atlantic cold anomaly in a global state estimate, *Ocean Sci.*, **18**, 953–978, <https://doi.org/10.5194/os-18-953-2022>, 2022.
- 1040 Schmale, J., Schneider, J., Nemitz, E., Tang, Y. S., Dragosits, U., Blackall, T. D., Trathan, P. N., Phillips, G. J., Sutton, M., and Braban, C. F.: Sub-Antarctic marine aerosol: dominant contributions from biogenic sources, *Atmos. Chem. Phys.*, **13**, 8669–8694, <https://doi.org/10.5194/acp-13-8669-2013>, 2013.



- 1045 Schneider, J., Freutel, F., Zorn, S. R., Chen, Q., Farmer, D. K., Jimenez, J. L., Martin, S. T., Artaxo, P., Wiedensohler, A., and Borrmann, S.: Mass-spectrometric identification of primary biological particle markers and application to pristine submicron aerosol measurements in Amazonia, *Atmos. Chem. Phys.*, 11, 11415–11429, <https://doi.org/10.5194/acp-11-11415-2011>, 2011.
- Schreiber, T.: Measuring Information Transfer, *Phys. Rev. Lett.*, 85, 461–464, <https://doi.org/10.1103/PhysRevLett.85.461>, 2000.
- 1050 Schwier, A. N., Rose, C., Asmi, E., Ebling, A. M., Landing, W. M., Marro, S., Pedrotti, M.-L., Sallon, A., Iuculano, F., Agusti, S., Tsiola, A., Pitta, P., Louis, J., Guieu, C., Gazeau, F., and Sellegri, K.: Primary marine aerosol emissions from the Mediterranean Sea during pre-bloom and oligotrophic conditions: correlations to seawater chlorophyll &lt;i>a</i> from a mesocosm study, *Atmos. Chem. Phys.*, 15, 7961–7976, <https://doi.org/10.5194/acp-15-7961-2015>, 2015.
- 1055 Seidel, M., Vemulapalli, S. P. B., Mathieu, D., and Dittmar, T.: Marine Dissolved Organic Matter Shares Thousands of Molecular Formulae Yet Differs Structurally across Major Water Masses, *Environ. Sci. Technol.*, 56, 3758–3769, <https://doi.org/10.1021/acs.est.1c04566>, 2022.
- 1060 Sellegri, K., Nicosia, A., Freney, E., Uitz, J., Thyssen, M., Grégori, G., Engel, A., Zäncker, B., Haëntjens, N., Mas, S., Picard, D., Saint-Macary, A., Peltola, M., Rose, C., Trueblood, J., Lefevre, D., D’Anna, B., Desboeufs, K., Meskhidze, N., Guieu, C., and Law, C. S.: Surface ocean microbiota determine cloud precursors, *Sci Rep*, 11, 281, <https://doi.org/10.1038/s41598-020-78097-5>, 2021.
- 1065 Sellegri, K., Harvey, M., Peltola, M., Saint-Macary, A., Barthelmeß, T., Rocco, M., Moore, K. A., Cristi, A., Peyrin, F., Barr, N., Labonnote, L., Marriner, A., McGregor, J., Safi, K., Deppeler, S., Archer, S., Dunne, E., Harnwell, J., Delanoë, J., Freney, E., Rose, C., Bazantay, C., Planche, C., Saiz-Lopez, A., Quintanilla-López, J. E., Lebrón-Aguilar, R., Rinaldi, M., Banson, S., Joseph, R., Lupascu, A., Jourdan, O., Mioche, G., Colomb, A., Olivares, G., Querel, R., McDonald, A., Plank, G., Bukosa, B., Dillon, W., Pelon, J., Baray, J.-L., Tridon, F., Donnadieu, F., Szczap, F., Engel, A., DeMott, P. J., and Law, C. S.: Sea2Cloud: From Biogenic Emission Fluxes to Cloud Properties in the Southwest Pacific, *Bulletin of the American Meteorological Society*, 104, E1017–E1043, <https://doi.org/10.1175/BAMS-D-21-0063.1>, 2023.
- 1070 Semper, S., Våge, K., Pickart, R. S., Jónsson, S., and Valdimarsson, H.: Evolution and Transformation of the North Icelandic Irminger Current Along the North Iceland Shelf, *JGR Oceans*, 127, e2021JC017700, <https://doi.org/10.1029/2021JC017700>, 2022.
- 1075 Simon, H., Bhave, P. V., Swall, J. L., Frank, N. H., and Malm, W. C.: Determining the spatial and seasonal variability in OM/OC ratios across the US using multiple regression, *Atmos. Chem. Phys.*, 11, 2933–2949, <https://doi.org/10.5194/acp-11-2933-2011>, 2011.
- Sinha, S., Sharma, H., and Shrivastava, M.: Application of advanced causal analyses to identify processes governing secondary organic aerosols, *Sci Rep*, 14, 10718, <https://doi.org/10.1038/s41598-024-59887-7>, 2024.
- 1080 Stein, A. F., Draxler, R. R., Rolph, G. D., Stunder, B. J. B., Cohen, M. D., and Ngan, F.: NOAA’s HYSPLIT Atmospheric Transport and Dispersion Modeling System, *Bulletin of the American Meteorological Society*, 96, 2059–2077, <https://doi.org/10.1175/BAMS-D-14-00110.1>, 2015.
- 1085 Ulbrich, I. M., Canagaratna, M. R., Zhang, Q., Worsnop, D. R., and Jimenez, J. L.: Interpretation of organic components from Positive Matrix Factorization of aerosol mass spectrometric data, *Atmos. Chem. Phys.*, 9, 2891–2918, <https://doi.org/10.5194/acp-9-2891-2009>, 2009.



- Van Alstyne, K. and Houser, L.: Dimethylsulfide release during macroinvertebrate grazing and its role as an activated chemical defense, *Mar. Ecol. Prog. Ser.*, 250, 175–181, <https://doi.org/10.3354/meps250175>, 2003.
- 1090 Veron, F.: Ocean Spray, *Annu. Rev. Fluid Mech.*, 47, 507–538, <https://doi.org/10.1146/annurev-fluid-010814-014651>, 2015.
- Villiermaux, E., Wang, X., and Deike, L.: Bubbles spray aerosols: Certitudes and mysteries, *PNAS Nexus*, 1, pgac261, <https://doi.org/10.1093/pnasnexus/pgac261>, 2022.
- 1095 Wang, Y., Zheng, X., Dong, X., Xi, B., Wu, P., Logan, T., and Yung, Y. L.: Impacts of long-range transport of aerosols on marine-boundary-layer clouds in the eastern North Atlantic, *Atmos. Chem. Phys.*, 20, 14741–14755, <https://doi.org/10.5194/acp-20-14741-2020>, 2020.
- Willis, M. D., Köllner, F., Burkart, J., Bozem, H., Thomas, J. L., Schneider, J., Aliabadi, A. A., Hoor, P. M., Schulz, H., Herber, A. B., Leaitch, W. R., and Abbatt, J. P. D.: Evidence for marine biogenic influence on summertime Arctic aerosol, *Geophys. Res. Lett.*, 44, 6460–6470, <https://doi.org/10.1002/2017GL073359>, 2017.
- 1100 Willoughby, A., Wozniak, A., and Hatcher, P.: Detailed Source-Specific Molecular Composition of Ambient Aerosol Organic Matter Using Ultrahigh Resolution Mass Spectrometry and <sup>1</sup>H NMR, *Atmosphere*, 7, 79, <https://doi.org/10.3390/atmos7060079>, 2016.
- 1105 Wolf, K. K. E., Hoppe, C. J. M., Rehder, L., Schaum, E., John, U., and Rost, B.: Heatwave responses of Arctic phytoplankton communities are driven by combined impacts of warming and cooling, *Sci. Adv.*, 10, ead15904, <https://doi.org/10.1126/sciadv.ad15904>, 2024.
- Xu, W., Lambe, A., Silva, P., Hu, W., Onasch, T., Williams, L., Croteau, P., Zhang, X., Renbaum-Wolff, L., Fortner, E., Jimenez, J. L., Jayne, J., Worsnop, D., and Canagaratna, M.: Laboratory evaluation of species-dependent relative ionization efficiencies in the Aerodyne Aerosol Mass Spectrometer, *Atmos. Chem. Phys.*, 18, 626–641, <https://doi.org/10.1080/02786826.2018.1439570>, 2018.
- 1110 Xu, W., Ovadnevaite, J., Fossum, K. N., Lin, C., Huang, R.-J., O’Dowd, C., and Ceburnis, D.: Aerosol hygroscopicity and its link to chemical composition in the coastal atmosphere of Mace Head: marine and continental air masses, *Atmos. Chem. Phys.*, 20, 3777–3791, <https://doi.org/10.5194/acp-20-3777-2020>, 2020.
- 1115 Xu, W., Fossum, K. N., Ovadnevaite, J., Lin, C., Huang, R.-J., O’Dowd, C., and Ceburnis, D.: The impact of aerosol size-dependent hygroscopicity and mixing state on the cloud condensation nuclei potential over the north-east Atlantic, *Atmos. Chem. Phys.*, 21, 8655–8675, <https://doi.org/10.5194/acp-21-8655-2021>, 2021.
- 1120 Yazdani, A., Dudani, N., Takahama, S., Bertrand, A., Prévôt, A. S. H., El Haddad, I., and Dillner, A. M.: Fragment ion–functional group relationships in organic aerosols using aerosol mass spectrometry and mid-infrared spectroscopy, *Atmos. Meas. Tech.*, 15, 2857–2874, <https://doi.org/10.5194/amt-15-2857-2022>, 2022.
- 1125 Zeppenfeld, S., Van Pinxteren, M., Hartmann, M., Zeising, M., Bracher, A., and Herrmann, H.: Marine Carbohydrates in Arctic Aerosol Particles and Fog – Diversity of Oceanic Sources and Atmospheric Transformations, *Aerosols/Field Measurements/Troposphere/Chemistry (chemical composition and reactions)*, <https://doi.org/10.5194/egusphere-2023-1607>, 2023.





- Zhang, Q., Jimenez, J. L., Canagaratna, M. R., Ulbrich, I. M., Ng, N. L., Worsnop, D. R., and Sun, Y.: Understanding atmospheric organic aerosols via factor analysis of aerosol mass spectrometry: a review, *Anal Bioanal Chem*, 401, 3045–3067, <https://doi.org/10.1007/s00216-011-5355-y>, 2011.
- 1130 Zhao, Z., He, Q., Lu, Z., Zhao, Q., and Wang, J.: Analysis of Atmospheric CO<sub>2</sub> and CO at Akedala Atmospheric Background Observation Station, a Regional Station in Northwestern China, *IJERPH*, 19, 6948, <https://doi.org/10.3390/ijerph19116948>, 2022.
- Zheng, G., Wang, Y., Wood, R., Jensen, M. P., Kuang, C., McCoy, I. L., Matthews, A., Mei, F., Tomlinson, J. M., Shilling, J. E., Zawadowicz, M. A., Crosbie, E., Moore, R., Ziemba, L., Andreae, M. O., and Wang, J.: New particle formation in the remote marine boundary layer, *Nat Commun*, 12, 527, 1135 <https://doi.org/10.1038/s41467-020-20773-1>, 2021.